

From fractal media to continuum mechanics

Martin Ostoj-Starzewski^{1,*}, Jun Li², Hady Joumaa³, and Paul N. Demmie⁴

¹ Department of Mechanical Science and Engineering, also Institute for Condensed Matter Theory and Beckman Institute, University of Illinois at Urbana-Champaign, Urbana, IL 61801, USA

² Division of Engineering and Applied Science, California Institute of Technology, Pasadena, CA 91125, USA

³ Department of Mechanical Science and Engineering, University of Illinois at Urbana-Champaign, Urbana, IL 61801, USA

⁴ Sandia National Laboratories Albuquerque, NM 87185, USA**

Received 30 August 2012, revised and accepted 17 December 2012

Published online 30 January 2013

Key words Fractals, continuum mechanics, dimensional regularization, balance laws.

This paper presents an overview of modeling fractal media by continuum mechanics using the method of dimensional regularization. The basis of this method is to express the balance laws for fractal media in terms of fractional integrals and, then, convert them to integer-order integrals in conventional (Euclidean) space. Following an account of this method, we develop balance laws of fractal media (continuity, linear and angular momenta, energy, and second law) and discuss wave equations in several settings (1d and 3d wave motions, fractal Timoshenko beam, and elastodynamics under finite strains). We then discuss extremum and variational principles, fracture mechanics, and equations of turbulent flow in fractal media. In all the cases, the derived equations for fractal media depend explicitly on fractal dimensions and reduce to conventional forms for continuous media with Euclidean geometries upon setting the dimensions to integers. We also point out relations and potential extensions of dimensional regularization to other models of microscopically heterogeneous physical systems.

© 2013 WILEY-VCH Verlag GmbH & Co. KGaA, Weinheim

1 Introduction

Natural or man-made objects are often broken or fractured in space or time and exhibit non-smooth or highly irregular features. Such objects are referred to as fractals, a term introduced by Benoît Mandelbrot [1]. Fractals in space include coastlines, porous media, cracks, turbulent flows, clouds, mountains, lightning bolts, snowflakes, melting ice, and even parts of living entities such as the neural structure or the surface of the human brain [2–4]. Fractals in time include signals, processes, and musical compositions. Geometric fractals exhibit a self-similarity property, that is, they appear similar at all levels of magnification. The Koch curve and the Cantor set are well-known examples of geometric fractals [2]. These fractal objects can be continuous or subdivided in parts, each of which is a reduced-size copy of the whole in a deterministic or stochastic sense. However, fractals encountered in real applications do not possess this powerful property of self-similarity. Nevertheless, they display a weaker or statistical version of self-similarity where randomness plays a key role in generating the body's geometry [4, 5]. For this reason, fractal models have been adopted to characterize random and even porous materials leading to mechanics based on fractal concepts [6, 7].

Mathematical fractal sets are characterized by the Hausdorff dimension D , which is the scaling exponent characterizing the fractal pattern's power law. For regular fractals, D is a constant and it is mathematically determined. But in the case of random fractals, D becomes a random variable and its evaluation is restricted to statistical methods [5]. Physical fractals can be modeled by mathematical ones only for some finite range of length scales within the lower and upper cutoffs. These objects are called pre-fractals [8]. The mechanics of fractal and pre-fractal media is still in a developing stage. It is inadequately explored and rarely utilized in comparison to continuum mechanics. Nevertheless, fractal mechanics can generate elegant models for problems where continuum mechanics fail particularly for bodies with highly irregular geometries [8–12].

Fundamental balance laws for fractals can be developed using a homogenization method called “dimensional regularization”. This paper is an overview of using this method to model fractal or pre-fractal media by continuum mechanics. With this method, fractional integrals over fractal sets are transformed to equivalent continuous integrals over Euclidean

* Corresponding author E-mail: martinost@illinois.edu

** Sandia National Laboratories is a multiprogram laboratory operated by Sandia Corporation, a Lockheed Martin Company, for the United States Department of Energy under Contract DE-AC04-94AL85000.

sets [13]. Dimensional regularization produces balance laws that are expressed in continuous form, thereby simplifying their mathematical manipulation both analytically and computationally. A product measure is used to achieve this transformation.

Tarasov used dimensional regularization to map a mechanics problem of a fractal onto a problem in the Euclidean space in which this fractal is embedded. He developed continuum-type equations for conservation of mass, linear momentum, and energy of fractals, and studied several fluid mechanics and wave problems [6, 7, 14, 15]. His approach to dimensional regularization of fractal objects employs fractional integrals in Euclidean space, a technique with its roots in quantum mechanics [16]. An advantage of this approach is that it admits upper and lower cutoffs of fractal scaling, so that one effectively deals with a physical pre-fractal rather than a purely mathematical fractal lacking any cutoffs.

The original formulation of Tarasov is based on the Riesz potential, which is more appropriate for isotropic fractal media than for anisotropic fractal media. To represent more general heterogeneous media, Li and Ostoja-Starzewski introduced a model that is based on a product measure [17–19]. Since this measure has different fractal dimensions in different directions, it grasps the anisotropy of fractal geometry better than the Tarasov formulation for a range of length scales between the lower and upper cutoffs [17, 19]. The great promise is that the conventional requirement of continuum mechanics, the separation of scales, can be removed with continuum-type field equations still employed. This approach was applied, among others, to thermomechanics with internal variables, extremum principles of elasticity and plasticity, turbulence in fractal porous media, dynamics of fractal beams, fracture mechanics and thermoelasticity [8–10, 13, 20].

2 Homogenization of fractal media via dimensional regularization

2.1 Mass power law and product measure

The basic approach to homogenization of fractal media by continua originated with Tarasov [6, 7, 15]. He worked in the setting where the mass obeys a power law

$$m(R) \sim R^D, \quad D < 3, \quad (2.1)$$

with R being the length scale of measurement (or resolution) and D the fractal dimension of mass. Note that the relation (2.1) can be applied to a *pre-fractal*, i.e., a fractal-type, physical object with lower and upper cutoffs. More specifically, Tarasov used a fractional integral to represent mass in a region \mathcal{W} embedded in the Euclidean three-space \mathbb{E}^3

$$m(\mathcal{W}) = \int_{\mathcal{W}} \rho(R) dV_D = \int_{\mathcal{W}} \rho(R) c_3(D, R) dV_3, \quad (2.2)$$

$$c_3(D, R) = R^{D-3} 2^{3-D} \Gamma(3/2) / \Gamma(D/2), \quad R = \sqrt{x_i x_i},$$

where \mathbf{R} is the position vector, R its magnitude, and Γ is the gamma function. Tarasov also defines the following transformation coefficients in the Riesz form

$$\begin{aligned} c_2(d, R) &= |\mathbf{R}|^{d-2} \frac{2^{2-d}}{\Gamma(d/2)}, \\ c_3(D, R) &= |\mathbf{R}|^{D-3} \frac{2^{3-D} \Gamma(3/2)}{\Gamma(D/2)}, \\ c(D, d, R) &= c_3^{-1}(D, R) c_2(d, R), \end{aligned} \quad (2.3)$$

and with them, the following operators (or, generalized derivatives) are used

$$\begin{aligned} \nabla_k^D f &= c_3^{-1}(D, R) \frac{\partial}{\partial x_k} [c_2(d, R) f] \equiv c_3^{-1}(D, R) \nabla_k [c_2(d, R) f], \\ \left(\frac{d}{dt} \right)_D f &= \frac{\partial f}{\partial t} + c(D, d, R) v_k \frac{\partial f}{\partial x_k}. \end{aligned} \quad (2.4)$$

In (2.2) and elsewhere we employ the Einstein summation convention unless otherwise stated.

The first and second equalities in (2.2)₁, respectively, involve fractional (Riesz-type) integrals and conventional integrals. In (2.2) the coefficient $c_3(D, R)$ provides a transformation between the two. dV_D is the infinitesimal volume element

in fractal space, and dV_3 is the infinitesimal volume element in \mathbb{E}^3 . Note that (2.2) expresses the idea of dimensional regularization in theoretical physics, which has its roots in regularizing integrals in the evaluation of Feynman diagrams [16]. For a function $f(x)$ this procedure is represented by

$$\int_W f(x) d^D x = \frac{2\pi^{D/2}}{\Gamma(D/2)} \int_0^\infty f(x) x^{D-1} dx. \quad (2.5)$$

That is, we begin with a fractal object embedded in \mathbb{E}^3 , whose spatial dimension is not 3 but rather some real number $D < 3$. The same is done with the surface of that object, which has its own fractal dimension d , with d not necessarily equal to $D - 1$. The balance laws are then written in weak forms involving volume and surface integrals over the fractal object. Converting these to conventional integrals via dimensional regularization, results, through localization, in strong forms for fractal bodies [15]. The key role in that approach is played by the Green-Gauss theorem for fractal media

$$\int_{\partial W} f_k n_k dS_d = \int_W c_3^{-1}(D, R) \nabla_k (c_2(d, R) f_k) dV_D, \quad (2.6)$$

where f_k is a vector field (in subscript notation) and

$$dS_d = c_2(d, R) dS_2 \quad dV_D = c_3(D, R) dV_3. \quad (2.7)$$

Thus, we can rewrite the fractional integrals in (2.6) as conventional ones

$$\int_{\partial W} c_2(d, R) f_k n_k dS_2 = \int_W \nabla_k (c_2(d, R) f_k) dV_3, \quad (2.8)$$

and, effectively, deal with formulas in (conventional) Euclidean setting, provided we have the coefficients c_3 and c_2 . Indeed, the latter are specified according to the fractional integral adopted.

Now, the above formulation has four drawbacks:

1. It involves a left-sided fractional derivative (Riemann-Liouville), which, when operating on a constant, does not generally give zero.
2. The mechanics-type derivation of wave equations yields a different result from the variational-type derivation.
3. The 3d (three-dimensional) wave equation does not reduce to the 1d wave equation.
4. It is limited to isotropic media.

The above issues motivated us to develop another formulation, which does not have these drawbacks. We outline this by first introducing a general anisotropic, fractal medium governed, in place of (2.1), by a more general power law relation with respect to each coordinate [17–19] (which, in fact, had originally been recognized by Tarasov)

$$m(L_1, L_2, L_3) \sim L_1^{\alpha_1} L_2^{\alpha_2} L_3^{\alpha_3}. \quad (2.9)$$

Then, the mass is specified via a *product measure*

$$m(\mathcal{W}) = \int_{\mathcal{W}} \rho(x_1, x_2, x_3) dl_{\alpha_1}(x_1) dl_{\alpha_2}(x_2) dl_{\alpha_3}(x_3), \quad (2.10)$$

while the length measure along each coordinate is given through transformation coefficients $c_1^{(k)}$

$$dl_{\alpha_k}(x_k) = c_1^{(k)}(\alpha_k, x_k) dx_k, \quad k = 1, 2, 3 \quad (\text{no sum}). \quad (2.11)$$

Equation (2.9) implies that the mass fractal dimension D equals $\alpha_1 + \alpha_2 + \alpha_3$ along the diagonals, $|x_1| = |x_2| = |x_3|$, where each α_k plays the role of a fractal dimension in the direction x_k . While it is noted that, in other directions the anisotropic fractal body's fractal dimension is not necessarily the sum of projected fractal dimensions, an observation from an established text on mathematics of fractals is recalled here [5]: "*Many fractals encountered in practice are not actually products, but are product-like.*" In what follows, we expect the equality between $D = \alpha_1 + \alpha_2 + \alpha_3$ to hold for fractals encountered in practice, whereas a rigorous proof of this property remains an open research topic.

2.2 Product measure

The relation (2.11) implies that the infinitesimal fractal volume element, dV_D , is

$$dV_D = dl_{\alpha_1}(x_1)dl_{\alpha_2}(x_2)dl_{\alpha_3}(x_3) = c_1^{(1)}c_1^{(2)}c_1^{(3)}dx_1dx_2dx_3 = c_3dV_3, \quad (2.12)$$

$$\text{with } c_3 = c_1^{(1)}c_1^{(2)}c_1^{(3)}.$$

For the surface transformation coefficient $c_2^{(k)}$, we consider a cubic volume element, $dV_3 = dx_1dx_2dx_3$, whose surface elements are specified by the normal vector along axes i, j , or k in Fig. 1. Therefore, $c_2^{(k)}$ associated with the surface $S_d^{(k)}$ is

$$c_2^{(k)} = c_1^{(i)}c_1^{(j)} = c_3/c_1^{(k)}, \quad i \neq j, \quad i, j \neq k. \quad (2.13)$$

The sum $d^{(k)} = \alpha_i + \alpha_j$, $i \neq j$, $i, j \neq k$, is the fractal dimension of the surface $S_d^{(k)}$ along the diagonals $|x_i| = |x_j|$ in $S_d^{(k)}$. This equality is not necessarily true elsewhere, but is expected to hold for fractals encountered in practice [5] as discussed previously for the relationship between D and $\alpha_1 + \alpha_2 + \alpha_3$.

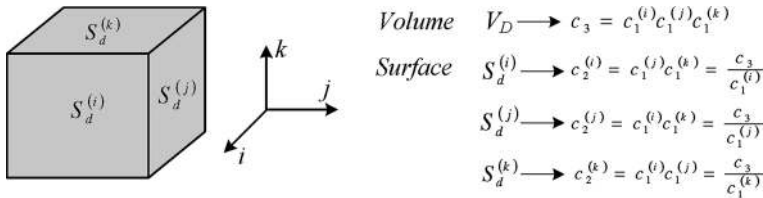


Fig. 1 Roles of the transformation coefficients $c_1^{(i)}$, $c_2^{(k)}$, and c_3 in homogenizing a fractal body of volume dV_D , surface dS_d , and lengths dl_α into a Euclidean parallelepiped of volume dV_3 , surface dS_2 , and length dx .

Figure 1 illustrates the relationship among the transformation coefficients $c_1^{(k)}$ and respective surface and volume transformation coefficients $c_2^{(k)}$, and c_3 which will be defined. We note that, when $D \rightarrow 3$ with each $\alpha_i \rightarrow 1$, the conventional concept of mass is recovered [21].

We adopt the modified Riemann-Liouville fractional integral of Jumarie [13, 22] for the transformation coefficients $c_1^{(k)}$,

$$c_1^{(k)} = \alpha_k \left(\frac{l_k - x_k}{l_{k0}} \right)^{\alpha_k - 1}, \quad k = 1, 2, 3, \quad (\text{no sum}), \quad (2.14)$$

where l_k is the total length (integral interval) along x_k and l_{k0} is the characteristic length in the given direction, like the mean pore size. In the product measure formulation, the resolution length scale is

$$R = \sqrt{l_k l_k}. \quad (2.15)$$

Let us examine $c_1^{(k)}$ in two special cases:

1. Uniform mass: The mass is distributed isotropically in a cubic region with a power law relation (2.9). Denoting the reference mass density by ρ_0 and the cubic length by l , we obtain

$$m(\mathcal{W}) = \rho_0 l^{\alpha_1} l^{\alpha_2} l^{\alpha_3} / l_0^{D-3} = \rho_0 l^{\alpha_1 + \alpha_2 + \alpha_3} / l_0^{D-3} = \rho_0 l^D / l_0^{D-3}, \quad (2.16)$$

which is consistent with the mass power law (2.1). In general, however, $D \neq \alpha_1 + \alpha_2 + \alpha_3$.

2. Point mass: The distribution of mass is concentrated at one point, so that the mass density is denoted by the Dirac function $\rho(x_1, x_2, x_3) = m_0 \delta(x_1) \delta(x_2) \delta(x_3)$. The fractional integral representing mass becomes

$$m(\mathcal{W}) = \alpha_1 \alpha_2 \alpha_3 \frac{l^{\alpha_1-1} l^{\alpha_2-1} l^{\alpha_3-1}}{l_0^{D-3}} m_0 = \alpha_1 \alpha_2 \alpha_3 \left(\frac{l}{l_0} \right)^{D-3} m_0, \quad (2.17)$$

When $D \rightarrow 3$ ($\alpha_1, \alpha_2, \alpha_3 \rightarrow 1$), $m(\mathcal{W}) \rightarrow m_0$ and the conventional concept of point mass is recovered [21]. Note that using the Riesz fractional integral is not well defined except when $D = 3$ (by letting $0^0 = 1$ in $m(\mathcal{W}) = \alpha_1 \alpha_2 \alpha_3 0^{D-3} m_0$), which on the other hand shows a non-smooth transition of mass with respect to its fractal dimension. This also supports our choice of the non-Riesz type expressions for $c_1^{(k)}$ in (2.14).

Note that the above expression for $c_1^{(k)}$ shows that the length dimension, and hence the mass m , would involve an unusual physical dimension if it were replaced by $c_1^{(k)} = \alpha_k (l_k - x_k)^{\alpha_k - 1}$. This behavior is understandable since, mathematically, a fractal curve only exhibits a finite measure with respect to a fractal dimensional length unit [1]. Of course, in practice, we prefer physical quantities to have usual dimensions, and so we work with non-dimensionalized coefficients $c_1^{(k)}$.

2.3 Carpinteri column

A simple generic example of an anisotropic, product-like fractal is the so-called *Carpinteri column* [23], a parallelepiped domain in \mathbb{E}^3 , having mathematically well defined Hausdorff dimensions in all three directions, Fig. 2. It has been proposed as a model of concrete columns which are essentially composite structures featuring oriented fractal-type microstructures. The square cross-section of the column is a *Sierpiński carpet*, which is “fractally” swept along the longitudinal direction in conjunction with a *Cantor ternary set*. The Hausdorff (fractal) dimension of this body along the longitudinal direction, x_3 , is that of the Cantor ternary set

$$D_3 = \frac{\ln 2}{\ln 3}. \quad (2.18)$$

On account of the axial and planar symmetries, the Hausdorff (fractal) dimension of the Sierpiński carpet is

$$D_{\text{carpet}} = \frac{\ln 8}{\ln 3}. \quad (2.19)$$

It follows that the Hausdorff (fractal) dimension for the entire column is

$$D_{\text{column}} = D_{\text{carpet}} + D_3 = 4 \frac{\ln 2}{\ln 3}. \quad (2.20)$$

Based on this idea, many other anisotropic fractals may be constructed.

It is important to note that, for the in-plane directions x_1 and x_2 ,

$$D_1 = D_2 = \frac{1}{3} \frac{\ln 18}{\ln 3}, \quad (2.21)$$

which is different from $\frac{1}{2} D_{\text{carpet}}$ which might be superficially assumed. The inapplicability of this simple supposition stems from the theory of products of fractal sets [5] which implies that, if a fractal set (denoted as G) is generated from the Cartesian product of two primary fractal sets (denoted as E and F), i.e. $G = E \times F$, their dimensions satisfy the following inequality (it becomes equality for continuous and Cantor sets),

$$D_G \geq D_E + D_F. \quad (2.22)$$

However, the Sierpiński carpet is not formed as the product of two independent fractal sets so that (2.22) cannot even predict an upper limit for D_1 .

2.4 Fractional integral theorems and fractal derivatives

In order to develop continuum mechanics of fractal media, we introduce the notion of fractal derivatives with respect to the coordinate x_k and time t . The definitions of these derivatives follow naturally from the fractional generalization of two basic integral theorems that are employed in continuum mechanics [14–16, 24]: Gauss theorem, which relates a volume integral to the surface integral over its bounding surface, and the Reynolds transport theorem, which provides an expression for the time rate of change of any volume integral in a continuous medium.

Consider the surface integral

$$\int_{\partial \mathcal{W}} \mathbf{f} \cdot \mathbf{n} dS_d = \int_{\partial \mathcal{W}} f_k n_k dS_d, \quad (2.23)$$

where $\mathbf{f} (= f_k)$ is any vector field and $\mathbf{n} (= n_k)$ is the outward normal vector field to the surface $\partial \mathcal{W}$ which is the boundary surface for some volume \mathcal{W} , and dS_d is the surface element in fractal space. The notation $(= A_k)$ is used to indicate that the A_k are components of the vector \mathbf{A} .

To compute (2.23), we relate the integral element $\mathbf{n}dS_d$ to its conventional surface element $\mathbf{n}dS_2$ in \mathbb{E}^3 via the fractal surface coefficients $c_2^{(k)}$, $k = 1, 2, 3$, as shown in Fig. 2. This figure shows that the infinitesimal element $\mathbf{n}dS_d$ can be expressed as a linear combination of the $n_k c_2^{(k)} dS_2$, $k = 1, 2, 3$ (no sum).

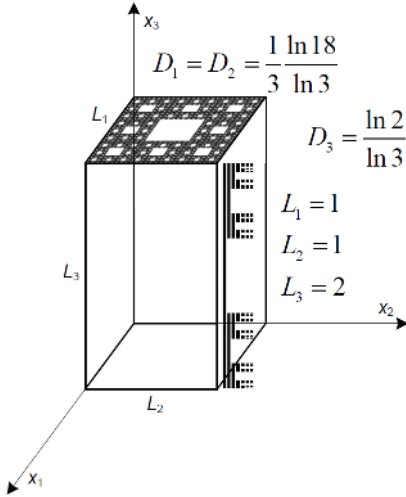


Fig. 2 The Carpinteri column with three fractal dimensions as explained in Sect. 2.3.

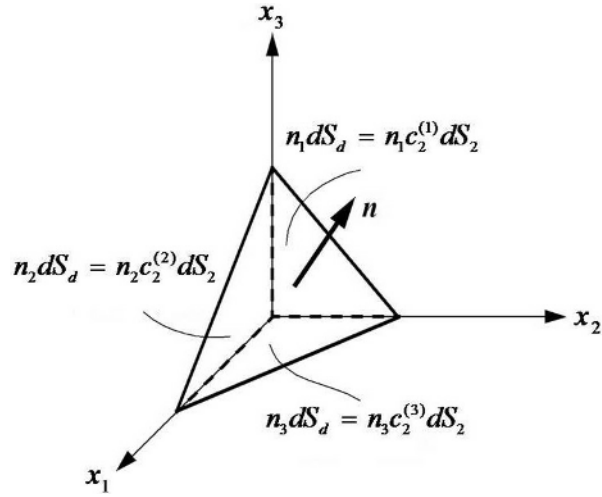


Fig. 3 Cauchy's tetrahedron of a fractal body interpreted via product measures.

By the conventional Gauss theorem, and noting that $c_2^{(k)}$ does not depend on the coordinate x_k , (2.23) becomes

$$\int_{\partial\mathcal{W}} \mathbf{f} \cdot \mathbf{n}dS_d = \int_{\partial\mathcal{W}} f_k n_k dS_d = \int_{\mathcal{W}} [f_k c_2^{(k)}]_{,k} dV_3 = \int_{\mathcal{W}} \frac{f_{k,k}}{c_1^{(k)}} dV_D. \quad (2.24)$$

In (2.24) and elsewhere, we employ the usual convention that $(\cdot)_{,k}$ is the partial derivative of (\cdot) with respect to x_k . Next, based on (2.11) and the above, we define the *fractal derivative* (*fractal gradient*), ∇_k^D as

$$\nabla_k^D = \frac{1}{c_1^{(k)}} \frac{\partial}{\partial x_k} \quad (\text{no sum}). \quad (2.25)$$

With this definition, the *Gauss theorem for fractal media* becomes

$$\int_{\partial\mathcal{W}} \mathbf{f} \cdot \mathbf{n}dS_d = \int_{\mathcal{W}} \nabla_k^D f_k dV_D = \int_{\mathcal{W}} (\nabla^D \cdot \mathbf{f}) dV_D. \quad (2.26)$$

It is straightforward to show that the fractal operator, ∇_k^D , commutes with the fractional integral operator; it is indeed its inverse and it satisfies the product rule for differentiation (the Leibnitz property). Furthermore, the fractal derivative of a constant is zero. This latter property shows that a fractal derivative and a fractional derivative are not the same since the fractional derivative of a constant does not always equal zero, neither in the fractional calculus [25] nor in Tarasov's formulation [15].

To define the fractal material time derivative, we consider the fractional generalization of Reynolds transport theorem. Consider any quantity, P , accompanied by a moving fractal material system, \mathcal{W}_t , with velocity vector field $\mathbf{v}(= v_k)$. The time derivative of the volume integral of P over \mathcal{W}_t is

$$\frac{d}{dt} \int_{\mathcal{W}_t} P dV_D. \quad (2.27)$$

Using the Jacobian (J) of the transformation between the current configuration (x_k) and the reference configuration (X_k), the relationship between the corresponding volume elements ($dV_D = J dV_D^0$), and the expression for the time derivative of J , it is straightforward to show that

$$\frac{d}{dt} \int_{\mathcal{W}_t} P dV_D = \int_{\mathcal{W}_t} \left[\frac{\partial P}{\partial t} + (v_k P)_{,k} \right] dV_D = \int_{\mathcal{W}_t} \left[\frac{\partial P}{\partial t} + c_1^{(k)} \nabla_k^D (v_k P) \right] dV_D. \quad (2.28)$$

The result given by the first equality is identical to the conventional representation. Hence, the fractal material time derivative and the conventional material time derivative are the same,

$$\left(\frac{d}{dt}\right)_D P = \frac{\partial P}{\partial t} + v_k P_{,k} = \frac{\partial P}{\partial t} + c_1^{(k)} v_k \nabla_k^D P. \quad (2.29)$$

Equation (2.29) is the *Reynolds theorem for fractal media*. While this form of the theorem is similar to the conventional form, an alternative form [17] of the fractional Reynolds transport theorem that involves surface integrals is different from the conventional one and rather complicated. This difference results from the fractal volume coefficient c_3 depending on all coordinates, whereas in the derivation of the fractional Gauss theorem, $c_2^{(k)}$ is independent of x_k .

2.5 Vector calculus on anisotropic fractals

Motivated by the preceding developments, we have the *fractal derivative (fractal gradient) operator* (grad)

$$\nabla^D \phi = \mathbf{e}_k \nabla_k^D \phi \quad \text{or} \quad \nabla_k^D \phi = \frac{1}{c_1^{(k)}} \frac{\partial \phi}{\partial x_k} \quad (\text{no sum on } k), \quad (2.30)$$

where \mathbf{e}_k is the base vector. Hence, the *fractal divergence* of a vector field

$$\text{div} \mathbf{f} = \nabla^D \cdot \mathbf{f} \quad \text{or} \quad \nabla_k^D f_k = \frac{1}{c_1^{(k)}} \frac{\partial f_k}{\partial x_k}. \quad (2.31)$$

This leads to a *fractal curl* operator of a vector field

$$\text{curl} \mathbf{f} = \nabla^D \times \mathbf{f} \quad \text{or} \quad e_{jki} \nabla_k^D f_i = e_{jki} \frac{1}{c_1^{(k)}} \frac{\partial f_i}{\partial x_k}. \quad (2.32)$$

The four fundamental identities of the conventional vector calculus can now be shown to carry over in terms of these new operators:

(i) The divergence of the curl of a vector field \mathbf{f} :

$$\text{div} \cdot \text{curl} \mathbf{f} = \mathbf{e}_m \nabla_m^D \cdot \mathbf{e}_j e_{jki} \nabla_k^D f_i = \frac{1}{c_1^{(j)}} \frac{\partial f}{\partial x_j} \left[e_{jki} \frac{1}{c_1^{(k)}} \frac{\partial f_i}{\partial x_k} \right] = 0, \quad (2.33)$$

where e_{ijk} is the permutation tensor.

(ii) The curl of the gradient of a scalar field ϕ :

$$\text{curl} \times (\text{grad} \phi) = \mathbf{e}_i e_{ijk} \nabla_j^D (\nabla_k^D \phi) = \mathbf{e}_i e_{ijk} \frac{1}{c_1^{(j)}} \frac{\partial}{\partial x_j} \left[\frac{1}{c_1^{(k)}} \frac{\partial \phi}{\partial x_k} \right] = 0. \quad (2.34)$$

In both cases above we can pull $1/c_1^{(k)}$ in front of the gradient because the coefficient $c_1^{(k)}$ is independent of x_j .

(iii) The divergence of the gradient of a scalar field ϕ is written in terms of the fractal gradient as

$$\text{div} \cdot (\text{grad} \phi) = \nabla_j^D \cdot \nabla_k^D \phi = \frac{1}{c_1^{(j)}} \frac{\partial}{\partial x_j} \left[\frac{1}{c_1^{(j)}} \frac{\partial \phi}{\partial x_j} \right] = \frac{1}{c_1^{(j)}} \left[\frac{\partial \phi_{,j}}{\partial x_j} \right]_{,j}, \quad (2.35)$$

which gives an explicit form of the *fractal Laplacian*.

(iv) The curl of the curl operating on a vector field \mathbf{f} :

$$\text{curl} \times (\text{curl} \mathbf{f}) = \mathbf{e}_p e_{prj} \nabla_r^D (e_{jki} \nabla_k^D f_i) = \mathbf{e}_p \nabla_r^D \left(\nabla_p^D f_r \right) - \mathbf{e}_p \nabla_r^D \nabla_r^D f_p. \quad (2.36)$$

Next, the Helmholtz decomposition for fractals can be proved along the classical lines: a vector field \mathbf{F} with known divergence and curl, none of which equal to zero, and which is finite, uniform and vanishes at infinity, may be expressed as the sum of a lamellar vector \mathbf{U} and a solenoidal vector \mathbf{V}

$$\mathbf{F} = \mathbf{U} + \mathbf{V} \quad (2.37)$$

with the operations

$$\text{curl} \mathbf{U} = \mathbf{0}, \quad \text{div} \mathbf{V} = 0 \quad (2.38)$$

understood in the sense of (2.32) and (2.31), respectively.

These results have recently been used [26] to obtain Maxwell equations modified to generally anisotropic fractal media using two independent approaches: a conceptual one (involving generalized Faraday and Ampère laws), and the one directly based on a variational principle for electromagnetic fields. In both cases the resulting equations are the same, thereby providing a self-consistent verification of our derivations. Just as Tarasov [15], we have found that the presence of anisotropy in the fractal structure leads to a source/disturbance as a result of generally unequal fractal dimensions in various directions. However, in the case of isotropy, our modified Maxwell equations do not exactly coincide with those of Tarasov.

2.6 Homogenization process for fractal media

The formula (2.10) for fractal mass expresses the mass power law using fractional integrals. From a homogenization standpoint, this relationship allows an interpretation of the fractal medium as an intrinsically discontinuous continuum with a fractal metric embedded in the equivalent homogenized continuum model as shown in Fig. 1. In this figure, dl_{α_i} , dS_d , dV_D represent the line, surface, and volume elements in the fractal medium, while dx_i , dS_2 , dV_3 , respectively, denote these elements in the homogenized continuum model. The coefficients $c_1^{(i)}$, $c_2^{(k)}$, c_3 provide the relationship between the fractal medium and the homogenized continuum model:

$$dl_{\alpha_i} = c_1^{(i)} dx_i, \quad dS_d = c_2^{(k)} dS_2, \quad dV_D = c_3 dV_3 \quad (\text{no sum}). \quad (2.39)$$

Standard image analysis techniques (such as the “box method” or the “sausage method” [27]) allow a quantitative calibration of these coefficients for every direction and every cross-sectional plane. In a non-fractal medium where all the c coefficients in (2.39) are unity, one recovers conventional forms of the transport and balance equations of continuum mechanics. As discussed in Sect. 3.3 below, the presence of fractal geometric anisotropy ($c_1^{(j)} \neq c_1^{(k)}$, $j \neq k$, in general), as reflected by differences between the α 's, leads to micropolar effects, see also [17, 18].

2.7 Discussion of calculus on fractals

The above formulations provide one choice of calculus on fractals, i.e. through fractional product integrals (2.10) to reflect the mass scaling law (2.9) of fractal media. The advantage of our approach is that it is connected with conventional calculus through coefficients c_1, c_2, c_3 and therefore well suited for development of continuum mechanics and partial differential equations on fractal media as we shall see in the next sections. Besides, the product formulation allows a decoupling of coordinate variables, which profoundly simplifies the Gauss theorem (2.26) and many results thereafter. We now investigate other choices of calculus on fractals to complement the proposed formulation.

To begin with, we define a mapping $P^\alpha : L \rightarrow m(L)$ that maps the length L to its mass m in fractal media with fractal dimension α ($0 < \alpha \leq 1$). The mass scaling law (2.9) requires the *fractality property* of P^α

$$P^\alpha(bL) = b^\alpha P^\alpha(L), \quad 0 < b \leq 1. \quad (2.40)$$

Note that the proposed fractional integral (2.10) is just one way to reflect this property. Now in an analogue of developing integrals on the real line, we decompose the fractal media into pieces and “combine” them together to recover the whole. But the fractality property does not allow a direct Riemann sum of each part. To illustrate this, considering a fractal of length L and fractal dimension α ($0 < \alpha \leq 1$), it follows that

$$P^\alpha\left(\frac{L}{2}\right) + P^\alpha\left(\frac{L}{2}\right) = \frac{P^\alpha(L)}{2^\alpha} + \frac{P^\alpha(L)}{2^\alpha} \neq P^\alpha(L). \quad (2.41)$$

We define an operator Λ^α on P^α satisfying the combination property:

$$P^\alpha(L) = \Lambda^\alpha [P^\alpha(l_1), P^\alpha(l_2), \dots, P^\alpha(l_n)], \quad l_i > 0, \quad \sum_{i=1}^n l_i = L. \quad (2.42)$$

Let $m = P^\alpha(L)$, $b_i = l_i/L$. Following the fractality property (2.40), we have

$$m = \Lambda^\alpha (b_1^\alpha m, b_2^\alpha m, \dots, b_n^\alpha m), \quad 0 < b_i \leq 1, \quad \sum_{i=1}^n b_i = 1. \quad (2.43)$$

A straightforward choice of Λ^α is an analogue of the p -norm in the L^p space:

$$\Lambda^\alpha(p_1, p_1, \dots, p_1) = \left(p_1^{1/\alpha} + p_2^{1/\alpha} + \dots + p_n^{1/\alpha} \right)^\alpha = \left(\sum_{i=1}^n p_i^{1/\alpha} \right)^\alpha. \quad (2.44)$$

In the limit $n \rightarrow \infty$, (2.44) induces another choice of P^α

$$P^\alpha(L) = m = \left[\int \rho(x)^{1/\alpha} dx \right]^\alpha, \quad (2.45)$$

where m is the mass of fractal media with length L and fractal dimension α ($0 < \alpha \leq 1$), and $\rho(x)$ is the local mass density; (2.45) is consistent with the fractality property (2.40). A generalization to 3d fractals follows similarly through product formulations. While we note that (2.45) cannot be transformed to conventional linear integrals through coefficients c_1, c_2, c_3 and the corresponding Gauss theorem is much more complicated.

The combination operator (2.44) suggests but one way to construct global forms based on established local formulations. To this end, we note that the proposed product measure is suitable for local properties of fractal media. The global formulation requires a nonlinear assembly of local forms through (2.44). To write it formally as

$$P^\alpha = \left[\int (dP^\alpha)^{1/\alpha} \right]^\alpha. \quad (2.46)$$

It is challenging to obtain analytical forms of global formulations, although we note that the discrete form can more easily be formulated in finite element implementations, where the assembly of elements is replaced by (2.46). In the following we shall discuss continuum mechanics based on the proposed local fractional integral (2.10). The assembly procedure and finite element implementations are not pursued further beyond this point.

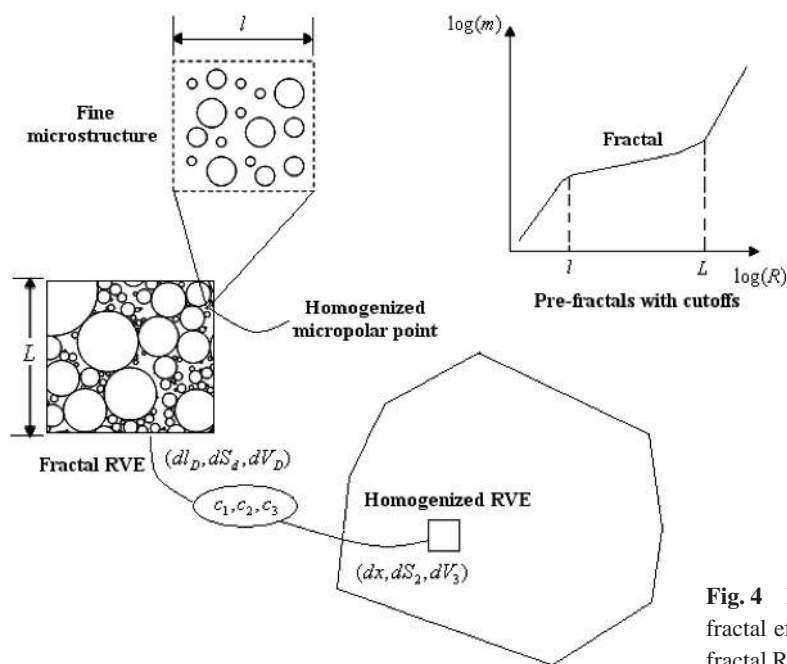


Fig. 4 Illustration of the two-level homogenization processes: fractal effects are present between the resolutions l and L in a fractal RVE with an Apollonian packing porous microstructure.

3 Continuum mechanics of fractal media

In the preceding section we discussed product measures and fractional integrals, generalized the Gauss and Reynolds theorems to fractal media, and introduced fractal derivatives. We now have the framework to develop continuum mechanics in a fractal setting. Here, the field equations for fractal media will be formulated analogously to the field equations of classical continuum mechanics, but will be based on fractional integrals and expressed in terms of fractal derivatives.

In light of the discussion in 2.6 between fractal media and classical continuum mechanics, the definitions of stress and strain are to be modified appropriately. First, we specify the relationship between surface force, $\mathbf{F}^S (= F_k^S)$, and the Cauchy

stress tensor, σ_{kl} , using fractional integrals as

$$F_k^S = \int_S \sigma_{lk} n_l dS_d, \quad (3.1)$$

where n_l are the components of the outward normal \mathbf{n} to S . On account of (2.39)₂, this force becomes

$$F_k^S = \int_S \sigma_{lk} n_l dS_d = \int_S \sigma_{lk} n_l c_2^{(l)} dS_2. \quad (3.2)$$

To specify the strain, we observe, using (2.39)₁ and the definition of a fractal derivative (2.25), that

$$\frac{\partial}{\partial l_{\alpha_k}} = \frac{\partial x_k}{\partial l_{\alpha_k}} \frac{\partial}{\partial x_k} = \frac{1}{c_1^{(k)}} \frac{\partial}{\partial x_k} = \nabla_k^D. \quad (3.3)$$

Thus, for small deformations, we define the strain, ε_{ij} , in terms of the displacement u_k as

$$\varepsilon_{ij} = \frac{1}{2} \left(\nabla_j^D u_i + \nabla_i^D u_j \right) = \frac{1}{2} \left[\frac{1}{c_1^{(j)}} u_{i,j} + \frac{1}{c_1^{(i)}} u_{j,i} \right] \quad (\text{no sum}). \quad (3.4)$$

As shown in [17], this definition of strain results in the same equations governing wave motion in linear elastic materials when derived by a variational approach as when derived by a mechanical approach, see Sect. 4.

In the following we apply the balance laws for mass, linear and angular momenta, energy, and entropy production to the fractal medium in order to derive the corresponding continuity equations.

3.1 Fractal continuity equation

Consider the equation for conservation of mass for \mathcal{W}

$$\frac{d}{dt} \int_{\mathcal{W}} \rho dV_D = 0, \quad (3.5)$$

where ρ is the density of the medium. Using the fractional Reynolds transport theorem (2.29), since \mathcal{W} is arbitrary, we find

$$\frac{\partial \rho}{\partial t} + (v_k \rho)_{,k} = \frac{d\rho}{dt} + \rho v_{k,k} = 0. \quad (3.6)$$

The *fractal continuity equation* follows when (3.6) is expressed in terms of the fractal derivative (3.3):

$$\frac{d\rho}{dt} + \rho c_1^{(k)} \nabla_k^D v_k = 0. \quad (3.7)$$

3.2 Fractal linear momentum equation

Consider the balance law of linear momentum for \mathcal{W} ,

$$\frac{d}{dt} \int_{\mathcal{W}} \rho \mathbf{v} dV_D = \mathbf{F}^B + \mathbf{F}^S, \quad (3.8)$$

where \mathbf{F}^B is the body force, and \mathbf{F}^S is the surface force given by (3.2). In terms of the components of velocity, v_k , and body force density, X_k , (3.8) can be written as

$$\frac{d}{dt} \int_{\mathcal{W}} \rho v_k dV_D = \int_{\mathcal{W}} X_k dV_D + \int_{\partial \mathcal{W}} \sigma_{lk} n_l dS_d. \quad (3.9)$$

Using the Reynolds transport theorem and the continuity equation (3.7), the left hand side is changed to

$$\frac{d}{dt} \int_{\mathcal{W}} \rho v_k dV_D = \int_{\mathcal{W}} \left[\frac{\partial \rho v_k}{\partial t} + (v_k v_l \rho)_{,l} \right] dV_D = \int_{\mathcal{W}} \rho \left[\frac{\partial v_k}{\partial t} + v_l v_{k,l} \right] dV_D = \int_{\mathcal{W}} \rho \frac{dv_k}{dt} dV_D. \quad (3.10)$$

Next, by the Gauss Theorem (2.26) and localization, we obtain the *fractal linear momentum equation*

$$\rho \dot{v}_k = X_k + \nabla_l^D \sigma_{lk}. \quad (3.11)$$

3.3 Fractal angular momentum equation

The conservation of angular momentum in a fractal medium is stated as

$$\frac{d}{dt} \int_{\mathcal{W}} \rho e_{ijk} x_j v_k dV_D = \int_{\mathcal{W}} e_{ijk} x_j X_k dV_D + \int_{\partial\mathcal{W}} e_{ijk} x_j \sigma_{lk} n_l dS_d. \quad (3.12)$$

Using (3.11) and the Gauss theorem (2.26) yields

$$e_{ijk} \frac{\sigma_{jk}}{c_1^{(j)}} = 0. \quad (3.13)$$

It was shown in [18, 19] that the presence of an anisotropic fractal structure is reflected by differences in the fractal dimensions α_i in different directions, which implies that $c_1^{(j)} \neq c_1^{(k)}$, $j \neq k$, in general. Therefore, the Cauchy stress is generally asymmetric in fractal media, suggesting that the micropolar effects should be accounted for and (3.12) should be augmented by the presence of couple-stresses. It is important to note here that a material may have anisotropic fractal structure, yet be isotropic in terms of its constitutive laws. This scenario will be pursued in Sect. 4.

Focusing now on physical fractals (so-called pre-fractals), we consider a body that obeys a fractal mass power law (2.4) between the lower and upper cutoffs. The choice of the continuum approximation is specified by the resolution R . Choosing the upper cut-off, we arrive at the fractal representative volume element (RVE) involving a region up to the upper cutoff, which is mapped onto a homogenized continuum element in the whole body. The micropolar point homogenizes the very fine microstructures into a rigid body (with 6 degrees of freedom) at the lower cutoff. The two-level homogenization processes are illustrated in Fig. 4.

To determine the inertia tensor \mathbf{I} at any micropolar point, we consider a rigid particle p having a volume \mathcal{P} , whose angular momentum is

$$\sigma_A = \int_{\mathcal{P}} (\mathbf{x} - \mathbf{x}_A) \times \mathbf{v}(\mathbf{x}, t) d\mu(\mathbf{x}). \quad (3.14)$$

Taking $\mathbf{v}(\mathbf{x}, t)$ as a helicoidal vector field (for some vector $\boldsymbol{\omega} \in \mathbb{R}^3$),

$$\mathbf{v}(\mathbf{x}, t) = \mathbf{v}(\mathbf{x}_A, t) + \boldsymbol{\omega} \times (\mathbf{x} - \mathbf{x}_A), \quad (3.15)$$

we have found [19] all (diagonal and off-diagonal) components of I_{kl} as

$$I_{kl} = \int_{\mathcal{P}} [x_m x_m \delta_{kl} - x_k x_l] \rho(\mathbf{x}) dV_D. \quad (3.16)$$

Here we use I_{kl} (Eringen uses i_{kl}) in the current state so as to distinguish it from I_{KL} in the reference state, the relation between both being given by [69]

$$I_{kl} = I_{KL} \chi_{kK} \chi_{lL}, \quad (3.17)$$

where χ_{kK} is a microdeformation tensor, or deformable director. For the entire fractal particle \mathcal{P} we have

$$\frac{d}{dt} \int_{\mathcal{P}} \rho I_{KL} dV_D = 0, \quad (3.18)$$

which, in view of (2.29), results in the *fractal conservation of microinertia*

$$\frac{d}{dt} I_{kl} = I_{kr} v_{lr} + I_{lr} v_{kr}. \quad (3.19)$$

In micropolar continuum mechanics [69], one needs a couple-stress tensor $\boldsymbol{\mu}$ and a rotation vector $\boldsymbol{\varphi}$ augmenting, respectively, the Cauchy stress tensor $\boldsymbol{\tau}$ (thus denoted so as to distinguish it from the symmetric $\boldsymbol{\sigma}$) and the deformation vector \mathbf{u} . The surface force and surface couple in the fractal setting can be specified by fractional integrals of $\boldsymbol{\tau}$ and $\boldsymbol{\mu}$, respectively, as

$$\mathbf{T}_k^S = \int_{\partial\mathcal{W}} \tau_{ik} n_i dS_d, \quad \mathbf{M}_k^S = \int_{\partial\mathcal{W}} \mu_{ik} n_i dS_d. \quad (3.20)$$

The above is consistent with the relation of force tractions and couple tractions to the force stresses and couple stresses on any surface element dS_d

$$t_k = \tau_{ik}n_i, \quad m_k = \mu_{ik}n_i. \quad (3.21)$$

Now, proceeding in a fashion similar as before, we obtain (3.11) plus the *fractal angular momentum equation*

$$\frac{e_{ijk}}{c_1^{(j)}} \tau_{jk} + \nabla_j^D \mu_{ji} + Y_i = I_{ij} \dot{w}_j. \quad (3.22)$$

In the above, Y_i is the body force couple, while $v_k (= \dot{u}_k)$ and $w_k (= \dot{\varphi}_k)$ are the deformation and rotation velocities, respectively.

3.4 Fractal energy equation

Globally, the conservation of energy has the following form

$$\frac{d}{dt} \int_{\mathcal{W}} (e + k) dV_D = \int_{\mathcal{W}} (X_i v_i + Y_i w_i) dV_D + \int_{\partial \mathcal{W}} (t_i v_i + m_i w_i - q_i n_i) dS_d, \quad (3.23)$$

where $k = \frac{1}{2} (\rho v_i v_i + I_{ij} w_i w_j)$ is the kinetic energy density, e the internal energy density, and $\mathbf{q} (= q_i)$ heat flux through the boundary of \mathcal{W} . As an aside we note that, just like in conventional (non-fractal media) continuum mechanics, the balance equations of linear momentum (3.11) and angular momentum (3.21) can be consistently derived from the invariance of energy (3.22) with respect to rigid body translations ($v_i \rightarrow v_i + b_i$, $w_i \rightarrow w_i$ and rotations ($v_i \rightarrow v_i + e_{ijk} x_j \omega_k$, $w_i \rightarrow w_i + \omega_i$), respectively.

To obtain the expression for the rate of change of internal energy, we start from

$$\int_{\mathcal{W}} (\dot{e} + \rho v_i \dot{v}_i + I_{ij} w_i \dot{w}_j) dV_D = \int_{\mathcal{W}} [X_i v_i + Y_i w_i + \nabla_j^D (\tau_{ji} v_j + \mu_{ji} w_j)] dV_D - \int_{\mathcal{W}} \nabla_i^D q_i dV_D, \quad (3.24)$$

and note (3.11) and (3.21), to find

$$\dot{e} = \tau_{ji} (\nabla_j^D v_i - e_{kji} w_k) + \mu_{ji} \nabla_j^D w_i - \nabla_i^D q_i. \quad (3.25)$$

Next, introducing the infinitesimal strain tensor and the curvature tensor in fractal media

$$\gamma_{ji} = \nabla_j^D u_i - e_{kji} \varphi_k, \quad \kappa_{ji} = \nabla_j^D \varphi_i, \quad (3.26)$$

we find that the energy balance (3.25) can be written as

$$\dot{e} = \tau_{ij} \dot{\gamma}_{ij} + \mu_{ij} \dot{\kappa}_{ij}. \quad (3.27)$$

Assuming e to be a state function of γ_{ij} and κ_{ij} only and assuming τ_{ij} and μ_{ij} not to be explicitly dependent on the temporal derivatives of γ_{ij} and κ_{ij} , we find

$$\tau_{ij} = \frac{\partial e}{\partial \gamma_{ij}}, \quad \mu_{ij} = \frac{\partial e}{\partial \kappa_{ij}}, \quad (3.28)$$

which shows that, just like in non-fractal continuum mechanics, also in the fractal setting (τ_{ij}, γ_{ij}) and (μ_{ij}, κ_{ij}) are conjugate pairs.

3.5 Fractal second law of thermodynamics

To derive the field equation of the second law of thermodynamics in a fractal medium $B(\omega)$, we begin with the global form of that law in the volume V_D , having a Euclidean boundary $\partial \mathcal{W}$, that is

$$\dot{S} = \dot{S}^{(r)} + \dot{S}^{(i)} \quad \text{with} \quad \dot{S}^{(r)} = \frac{\dot{Q}}{T}, \quad \dot{S}^{(i)} \geq 0, \quad (3.29)$$

where \dot{S} , $\dot{S}^{(r)}$, and $\dot{S}^{(i)}$ stand, respectively, for the total, reversible, and irreversible entropy production rates in V_D . Equivalently,

$$\dot{S} \geq \dot{S}^{(r)}. \quad (3.30)$$

Thus, we can write (3.30) as

$$\frac{d}{dt} \int_W \rho s \, dV_D = \dot{S} \geq \dot{S}^{(r)} = - \int_{\partial W} \frac{q_k n_k}{T} dS_d, \quad (3.31)$$

which, on account of (2.29), may be re-written as

$$\int_W \rho \frac{d}{dt} s \, dV_D \geq - \int_W \nabla_k^D \left(\frac{q_k}{T} \right) dV_D, \quad (3.32)$$

so as to result in a local form of the second law

$$\rho \frac{ds}{dt} \geq - \nabla_k^D \left(\frac{q_k}{T} \right), \quad (3.33)$$

or, more explicitly,

$$\rho \frac{ds}{dt} \geq - \frac{\nabla_k^D q_{k,k}}{T} + \frac{q_k \nabla_k^D T}{T^2}. \quad (3.34)$$

Just like in thermomechanics of non-fractal bodies [28], we now introduce the rate of irreversible entropy production $\rho \dot{S}^{(i)}$ which, in view of (3.34), gives

$$0 \leq \rho \dot{S}^{(i)} = \rho \dot{s} + \frac{\nabla_k^D q_{k,k}}{T} - \frac{q_k \nabla_k^D T}{T^2} + \rho h. \quad (3.35)$$

Here with s we denote specific entropies (i.e. per unit mass). Next, we recall the classical relation between the free energy density ψ , the internal energy density e , the entropy s , and the absolute temperature T : $\psi = e - Ts$. This allows us to write for time rates of these quantities

$$\dot{\psi} = \dot{e} - s\dot{T} - T\dot{s}. \quad (3.36)$$

On the other hand, with ψ being a function of the strain γ_{ji} and curvature-torsion κ_{ji} tensors, the internal variables α_{ij} (strain type) and ζ_{ij} (curvature-torsion type), and temperature T , we have

$$\rho \dot{\psi} = \rho \frac{\partial \psi}{\partial \gamma_{ij}} \dot{\gamma}_{ij} + \rho \frac{\partial \psi}{\partial \alpha_{ij}} \dot{\alpha}_{ij} + \rho \frac{\partial \psi}{\partial \kappa_{ij}} \dot{\kappa}_{ij} + \rho \frac{\partial \psi}{\partial \zeta_{ij}} \dot{\zeta}_{ij} + \rho \frac{\partial \psi}{\partial T} \dot{T}. \quad (3.37)$$

In the above we shall adopt the conventional relations giving the (external and internal) quasi-conservative Cauchy and Cosserat (couple) stresses as well as the entropy density as gradients of ψ

$$\tau_{ij}^{(q)} = \rho \frac{\partial \psi}{\partial \varepsilon_{ij}}, \quad \beta_{ij}^{(q)} = \rho \frac{\partial \psi}{\partial \alpha_{ij}}, \quad \mu_{ij}^{(q)} = \rho \frac{\partial \psi}{\partial \kappa_{ij}}, \quad \eta_{ij}^{(q)} = \rho \frac{\partial \psi}{\partial \zeta_{ij}}, \quad s = - \frac{\partial \psi}{\partial T}. \quad (3.38)$$

This is accompanied by a split of total Cauchy and micropolar stresses into their quasi-conservative and dissipative parts

$$\tau_{ij} = \tau_{ij}^{(q)} + \tau_{ij}^{(d)}, \quad \mu_{ij} = \mu_{ij}^{(q)} + \mu_{ij}^{(d)}, \quad (3.39)$$

along with relations between the internal quasi-conservative and dissipative stresses

$$\beta_{ij}^{(q)} = -\beta_{ij}^{(d)}, \quad \eta_{ij}^{(q)} = -\eta_{ij}^{(d)}. \quad (3.40)$$

In view of (3.36-38), we obtain

$$\rho \left(\dot{\psi} + s\dot{T} \right) = \rho (\dot{e} - T\dot{s}) = \tau_{ij}^{(q)} \dot{\gamma}_{ij} + \beta_{ij}^{(q)} \dot{\alpha}_{ij} + \mu_{ij}^{(q)} \dot{\kappa}_{ij} + \eta_{ij}^{(q)} \dot{\zeta}_{ij} + \rho h. \quad (3.41)$$

On account of the energy balance, this is equivalent to

$$T\rho\dot{s} = \tau_{ij}^{(d)}\dot{\gamma}_{ij} + \beta_{ij}^{(d)}\dot{\alpha}_{ij} + \mu_{ij}^{(d)}\dot{\kappa}_{ij} + \eta_{ij}^{(d)}\dot{\zeta}_{ij} - \nabla_k^D q_k + \rho h. \quad (3.42)$$

Recalling (3.35), we find the local form of the second law in terms of time rates of strains and internal parameters

$$0 \leq T\rho\dot{s}^{(i)} = \tau_{ij}^{(d)}\dot{\gamma}_{ij} + \beta_{ij}^{(d)}\dot{\alpha}_{ij} + \mu_{ij}^{(d)}\dot{\kappa}_{ij} + \eta_{ij}^{(d)}\dot{\zeta}_{ij} - \frac{q_k \nabla_k^D T}{T} + \rho h. \quad (3.43)$$

The above is a generalization of the Clausius-Duhem inequality to fractal dissipative media with internal parameters. Upon dropping the internal parameters (which may well be the case for a number of materials), the terms $\beta_{ij}^{(d)}\dot{\alpha}_{ij}$ and $\eta_{ij}^{(d)}\dot{\zeta}_{ij}$ drop out, whereas, upon neglecting the micropolar effects, the terms $\mu_{ij}^{(d)}\dot{\kappa}_{ij}$ and $\eta_{ij}^{(d)}\dot{\zeta}_{ij}$ drop out.

For non-fractal bodies, the stress tensor τ_{ij} reverts back to σ_{ij} , and (3.43) reduces to the simple well-known form [28]

$$0 \leq T\rho\dot{s}^{(i)} = \sigma_{ij}^{(d)}\dot{\gamma}_{ij} - \frac{T_k q_k}{T} + \rho h. \quad (3.44)$$

It is most interesting that the fractal derivative of (2.25) appears only in the thermal dissipation term. In fact, this derivative arises in processes of heat transfer in a fractal rigid conductor and coupled thermoelasticity of fractal deformable media [20].

4 Fractal wave equations

Just like in conventional continuum mechanics, the basic continuum equations for fractal media presented above have to be augmented by constitutive relations. At this point, we expect that the fractal geometry influences configurations of physical quantities like stress and strain, but does not affect the physical laws (like conservation principles) and constitutive relations that are inherently due to material properties. This expectation is supported in two ways:

- a study of scale effects of material strength and stress from the standpoint of fractal geometry which is confirmed by experiments involving both brittle and plastic materials [29];
- derivations of wave equations through mechanical and variational approaches, respectively [24], as shown below.

4.1 1d wave motion

The 1d plane wave motion [$u \equiv u_1(x_1)$, $\phi_i \equiv 0$] involves one spatial variable only: $x \equiv x_1$. First, using the mechanical approach, we begin from the balance of linear momentum (3.11), along with Hooke's law $\sigma = E\varepsilon$ (E being Young's modulus) to get

$$\rho\ddot{u} = E\nabla^D \varepsilon. \quad (4.1)$$

Following the conventional strain definition, $\varepsilon = \nabla u$, gives ($c_1 \equiv c_1^{(1)}$)

$$\rho\ddot{u} = E\nabla^D \nabla u \equiv E c_1^{-1} (u_{,x})_{,x} \quad (4.2)$$

whereas, following our fractal definition of strain (3.4) simplified to 1d, $\varepsilon = \nabla^D u$, yields

$$\rho\ddot{u} = E\nabla^D \nabla^D u \equiv E c_1^{-1} (c_1^{-1} u_{,x})_{,x}. \quad (4.3)$$

Now, using the variational approach we begin from Hamilton's principle that involves the Lagrangian function $L = \mathcal{K} - \mathcal{E}$, where (with $dl_D = c_1 dx$)

$$\mathcal{K} = \frac{1}{2}\rho \int \dot{u}^2 dl_D = \frac{1}{2}\rho \int \dot{u}^2 c_1 dx, \quad \mathcal{E} = \frac{1}{2}E \int u^2 dl_D = \frac{1}{2}E \int u^2 c_1 dx. \quad (4.4)$$

Following the conventional strain definition, $\varepsilon = \nabla u$, gives

$$\rho\ddot{u} = E c_1^{-1} (c_1 u_{,x})_{,x} \quad (4.5)$$

whereas, following our definition (3.4) simplified to 1d, $\varepsilon = \nabla^D u$, yields

$$\rho\ddot{u} = E c_1^{-1} (c_1^{-1} u_{,x})_{,x}. \quad (4.6)$$

A comparison of the results among the mechanical and variational approaches, we find that (4.6) agrees with (4.3), while (4.5) contradicts (4.2), showing that our definitions of fractal stress and strain are self-consistent [17]. Precisely the same type of results have also been obtained for 2d anti-plane waves, 3d waves, as well as the Timoshenko beam elastodynamics (discussed below).

Upon considering harmonic motions $u(x, t) = U(x) e^{j\omega t}$, (4.6) leads to a 1d fractal Helmholtz equation

$$0 = k^2 U + \nabla^D \nabla^D U \equiv k^2 U + c_1^{-1} (c_1^{-1} U_{,x})_{,x} \quad (4.7)$$

where $k = \omega/\vartheta$ is the wavenumber, $\vartheta = \sqrt{E/\rho}$ being the wave speed. Assuming the motion to occur on the interval $[0, L]$, results in

$$-\left(\frac{U'}{c_1}\right)' = c_1 k^2 U \quad \text{or} \quad (4.8)$$

$$(L-x)^2 U''(x) + (D-1)(L-x)U'(x) + k^2 D^2 (L-x)^{2D} U(x) = 0.$$

This modal equation admits the general solutions in terms of *fractal harmonics* (Fig. 5)

$$f_1(x, k) = \cos[k(L-x)^D], \quad f_2(x, k) = \sin[k(L-x)^D], \quad (4.9a)$$

so that the modal function for a given boundary value problem (BVP) can be expressed as

$$U_n(x) = C_1 f_1(x, k_n) + C_2 f_2(x, k_n), \quad (4.10)$$

where the constants C_1 and C_2 are determined from the appropriate boundary conditions (BC).

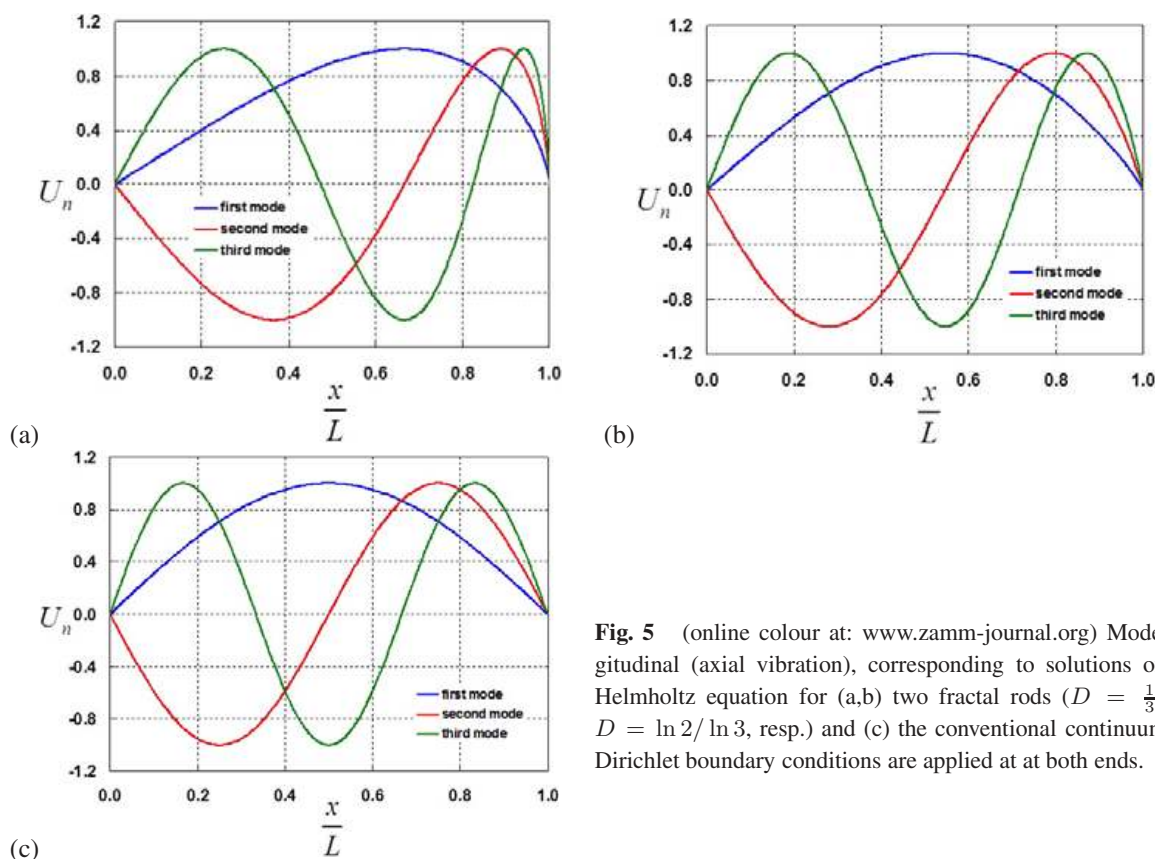


Fig. 5 (online colour at: www.zamm-journal.org) Mode shapes in longitudinal (axial vibration), corresponding to solutions of the 1d fractal Helmholtz equation for (a,b) two fractal rods ($D = \frac{1}{3} \ln 18 / \ln 3$ and $D = \ln 2 / \ln 3$, resp.) and (c) the conventional continuum rod ($D = 1$). Dirichlet boundary conditions are applied at both ends.

4.2 3d wave motion

Assuming a micropolar material of linear elastic and centrosymmetric type, its energy density is given by a scalar product

$$e = \frac{1}{2} \gamma_{ij} C_{ijkl}^{(1)} \gamma_{kl} + \frac{1}{2} \kappa_{ij} C_{ijkl}^{(2)} \kappa_{kl}, \quad (4.11)$$

so that the pertinent Hooke law is

$$\tau_{ij} = C_{ijkl}^{(1)} \gamma_{kl}, \quad \mu_{ij} = C_{ijkl}^{(2)} \kappa_{kl}. \quad (4.12)$$

Here $C_{ijkl}^{(1)}$ and $C_{ijkl}^{(2)}$ are two micropolar stiffness tensors. Note that, due to the existence of e , we have the basic symmetry of both stiffness (and hence, compliance) tensors

$$C_{ijkl}^{(1)} = C_{klij}^{(1)}, \quad C_{ijkl}^{(2)} = C_{klij}^{(2)}. \quad (4.13)$$

Focusing henceforth on the centrosymmetric case, for an elastically isotropic material, the tensors $C_{ijkl}^{(1)}$ and $C_{ijkl}^{(2)}$ become

$$\begin{aligned} C_{ijkl}^{(1)} &= (\mu - \alpha) \delta_{jk} \delta_{il} + (\mu + \alpha) \delta_{jl} \delta_{ik} + \lambda \delta_{ij} \delta_{kl}, \\ C_{ijkl}^{(2)} &= (\gamma - \varepsilon) \delta_{jk} \delta_{il} + (\gamma + \varepsilon) \delta_{jl} \delta_{ik} + \beta \delta_{ij} \delta_{kl}. \end{aligned} \quad (4.14)$$

Here λ and μ are the Lamé constants of classical elasticity, while α , β , γ , and ε are the micropolar constants. Note that this nomenclature is consistent with that employed by Nowacki [30], whereas μ , γ , and β were denoted, respectively, by β , ψ , and η in [31]. With the mass moment of inertia $I_{ij} = \delta_{ij} I$, it follows that the equations of elastodynamics in displacements and rotations are

$$\begin{aligned} \rho \ddot{u}_i &= (\mu + \alpha) \left[\nabla_j^D \nabla_j^D u_i - \nabla_j^D \left(e_{kji} \frac{\phi_k}{c_1^{(j)}} \right) \right] + (\mu - \alpha + \lambda) \nabla_i^D \nabla_j^D u_j + (\mu - \alpha) \nabla_j^D \left(e_{kij} \frac{\phi_k}{c_1^{(i)}} \right), \\ I \ddot{\phi}_i &= (\gamma + \varepsilon) \nabla_j^D \nabla_j^D \phi_i + (\psi - \varepsilon + \beta) \nabla_i^D \nabla_j^D \phi_j \\ &\quad - (\mu + \alpha) \left[\phi_i \sum_{j \neq i} \frac{1}{c_1^{(j)} c_1^{(j)}} + e_{ijk} \frac{\nabla_j^D u_k}{c_1^{(j)}} \right] + (\mu - \alpha) e_{ijk} \frac{\nabla_k^D u_j}{c_1^{(j)}} + 2(\mu - \alpha) \frac{\phi_i u_i}{c_3}. \end{aligned} \quad (4.15)$$

In [31, 32] we have explored the elastodynamics in micropolar fractal solids from both analytical and computational perspectives. The analytical approach is feasible only for some particular problems discussed below, and classified in vein of [30].

4.2.1 3d dilatational wave motion

As a very special case, it is possible for the above model to involve no rotational degrees of freedom with the couple stress μ being identically zero everywhere, while simultaneously satisfying the angular momentum balance. This occurs by setting all the shear components of the stress tensor σ to be identically zero i.e. $\sigma_{ij} \equiv 0$ for $i \neq j$ and prescribing the motion such that the displacement in a given direction depends only on the coordinate of that direction

$$u_i \equiv u_i(x_i) \quad i = 1, \dots, 3. \quad (4.16)$$

The wave motion is then of dilatational or primary type [33]. Now, the incorporation of isotropic Hooke's law $\sigma_{ij} = \lambda \epsilon_{kk} \delta_{ij} + 2\mu \epsilon_{ij}$ into the linear momentum balance produces the fractal Navier equation, characterized by three generally different fractal dimensions,

$$\rho \ddot{u}_i = \frac{\lambda + \mu}{c_3} \left(\frac{c_3 u_{j,i}}{c_1^{(i)} c_1^{(j)}} \right)_{,j} + \frac{\mu}{c_3} \left(\frac{c_3 u_{i,j}}{c_1^{(j)} c_1^{(j)}} \right)_{,j}. \quad (4.17)$$

In contradistinction to the continuum case, Eq. (4.17) is only meaningful to study dilatational wave propagation problems. On account of (4.17), we have a set of three decoupled equations, the first being

$$\frac{\rho \ddot{u}_1}{\lambda + 2\mu} = \frac{u_{1,11}}{c_1^2} - \frac{c_{1,1} u_{1,1}}{c_1^3}, \quad (4.18)$$

with the next two obtained by cyclic permutations $1 \rightarrow 2 \rightarrow 3$; note that the above is identical to (4.6). The decoupling of wave motions in three orthogonal directions allows the solution of a 3d problem via three similar problems of 1d type. This significantly simplifies the computational analysis.

With reference to the 1d fractal Helmholtz equation, in the case of homogeneous BC, the Sturm-Liouville problem (4.8) admits the following modal orthonormality property

$$\int_0^L U_m(x) U_n(x) c_1(x) dx = \delta_{mn}. \quad (4.19)$$

Next, three BVP have been studied in detail in [32]: Dirichlet, first mixed, and second mixed. Also, a finite element method (FEM) has been shown to be robust in handling mechanics problems in fractal solids. Indeed, in the 1d case, using admissible functions $\hat{u} \in H^1(\Omega)$, $\Omega = [0, L]$, from (4.18) we obtain the weak form

$$\int_{\Omega} \rho c \ddot{u} \hat{u} d\Omega + \int_{\Omega} (\lambda + 2\mu) \frac{u_{,x} \hat{u}_{,x}}{c} d\Omega = 0. \quad (4.20)$$

Upon partitioning the domain Ω into a countable union of finite elements Ω_e (where $\bigcup_e \Omega_e = \Omega$), we obtain a discrete formulation

$$\mathbf{M} \cdot \ddot{\mathbf{U}} + \mathbf{K} \cdot \mathbf{U} = 0, \quad (4.21)$$

where, on the elemental level, the inertia and stiffness matrices are evaluated as

$$M_{ij}^e = \int_{\Omega_e} \rho c h_i h_j dx, \quad K_{ij}^e = \int_{\Omega_e} (\lambda + 2\mu) \frac{h_{i,x} h_{j,x}}{c} dx. \quad (4.22)$$

The governing matrices are symmetric; they can be evaluated exactly without performing any numerical integration (e.g. Gaussian quadrature rule). The trapezoidal time stepping method is implemented to determine the transient solution [34]. This time march scheme is implicit, unconditionally stable and second-order accurate.

4.2.2 Torsional wave problem

Consider the problem where the displacement is suppressed to zero and the microrotation is permitted in such a way that every rotation solely depends on the direction about which it occurs. Mathematically, we have

$$u_i \equiv 0, \quad \phi_i \equiv \phi_i(x_i). \quad (4.23)$$

Here the shear components of the curvature and couple-stress tensors are all identically zero. The axial components of the strain and stress tensors are zero too (rendering the deformation equivoluminal), but not the shear components. As a result, the elastodynamic equations for the rotation field cannot be solved exactly unless certain restrictions on the elastic moduli are enforced. For example, considering the governing equation for ϕ_1 , we have

$$I \ddot{\phi}_1 = (2\gamma + \beta) \nabla_1^D (\nabla_1^D \phi_1) + \phi_1 \left[2 \frac{\mu - \alpha}{c_1^{(2)} c_1^{(3)}} - (\mu + \alpha) \left(\frac{1}{[c_1^{(2)}]^2} + \frac{1}{[c_1^{(3)}]^2} \right) \right]. \quad (4.24)$$

The general solution can be given in terms of the fractal harmonics introduced earlier.

4.2.3 In-plane problem

This is a generalization of the in-plane elasticity where the displacement and the rotation fields are prescribed as

$$\begin{aligned} u_1 &\equiv u_1(x_1), & u_2 &\equiv u_2(x_i), & u_3 &\equiv 0, \\ \phi_1 &\equiv 0, & \phi_2 &\equiv 0, & \phi_3 &\equiv \phi_3(x_1, x_2). \end{aligned} \quad (4.25)$$

By examining the strain and curvature tensors and, in turn, the constitutive relations, we find the linear momentum equations for u_1 and u_2 along with the angular momentum equation for ϕ_3

$$\begin{aligned}\rho\ddot{u}_1 &= (2\mu + \lambda) \nabla_1^D \nabla_1^D u_1 + (\mu - \alpha) \nabla_2^D \left(\frac{-\phi_3}{c_1^{(1)}} \right) + (\mu + \alpha) \nabla_2^D \left(\frac{\phi_3}{c_1^{(2)}} \right), \\ \rho\ddot{u}_2 &= (2\mu + \lambda) \nabla_2^D \nabla_2^D u_2 + (\mu - \alpha) \nabla_1^D \left(\frac{\phi_3}{c_1^{(2)}} \right) + (\mu + \alpha) \nabla_1^D \left(\frac{-\phi_3}{c_1^{(1)}} \right), \\ I\ddot{\phi}_3 &= (\gamma + \epsilon) \left[\nabla_1^D \nabla_1^D \phi_3 + \nabla_2^D \nabla_2^D \phi_3 \right] - (\mu + \alpha) \left[\frac{1}{[c_1^{(2)}]^2} + \frac{1}{[c_1^{(1)}]^2} \right] \phi_3 + (\mu - \alpha) \frac{\phi_3}{c_1^{(1)} c_1^{(2)}}.\end{aligned}\quad (4.26)$$

Upon setting $\alpha = \mu = 0$, the displacements are found to be governed by the 1d fractal wave equations, while ϕ_3 by a 2d fractal wave equation

$$I\ddot{\phi}_3 = (\gamma + \epsilon) \left[\nabla_1^D \nabla_1^D \phi_3 + \nabla_2^D \nabla_2^D \phi_3 \right]. \quad (4.27)$$

Turning to harmonic wave motions ($\phi_3(x, t) = \Phi_3(x_1, x_2)e^{j\omega t}$), we arrive at a 2d fractal Helmholtz equation

$$0 = k^2 \Phi_3 + \nabla_1^D \nabla_1^D \Phi_3 + \nabla_2^D \nabla_2^D \Phi_3, \quad (4.28)$$

where $k = \omega/\vartheta$ is the wavenumber, $\vartheta = \sqrt{(\gamma + \beta)/I}$. Figure 6 displays contour plots for the first few modes of Φ_3 on the Sierpiński carpet under the Dirichlet BC on its entire boundary. Again, solutions of the BVP can be given in terms of fractal harmonics.

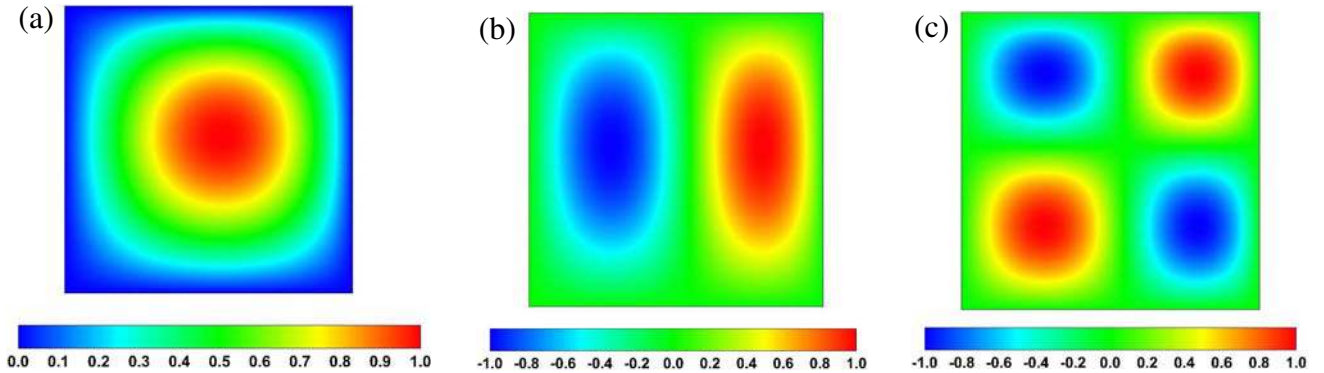


Fig. 6 (online colour at: www.zamm-journal.org) Some basic mode shapes corresponding to solutions of the 2d fractal Helmholtz equation where $L_1 = L_2 = 1$ and $D_1 = D_2 = \ln 18/(3 \ln 3)$. (a) $n_1 = 1, n_2 = 1$. (b) $n_1 = 2, n_2 = 1$. (c) $n_1 = 2, n_2 = 2$.

4.2.4 Out-of-plane problem

In this second planar problem – actually, a generalization of the out-of-plane elasticity – the in-plane rotations depend on the in-plane coordinates while the out-of-plane displacement on x_3 :

$$\begin{aligned}u_1 &\equiv 0, \quad u_2 \equiv 0, \quad u_3 \equiv u_1(x_1, x_2, x_3), \\ \phi_1 &\equiv \phi_1(x_1, x_2), \quad \phi_2 \equiv \phi_1(x_1, x_2), \quad \phi_3 \equiv 0.\end{aligned}\quad (4.29)$$

By following a route analogous to those outlined above, and assuming $\gamma - \epsilon + \beta = 0$, we arrive at a system of decoupled equations for ϕ_1 and ϕ_2

$$\begin{aligned}\rho\ddot{u}_3 &= \lambda \nabla_3^D \nabla_3^D u_3, \\ I\ddot{\phi}_1 &= (\beta + 2\gamma) \left[\nabla_1^D \nabla_1^D \phi_1 + \nabla_2^D \nabla_2^D \phi_1 \right], \\ I\ddot{\phi}_2 &= (\beta + 2\gamma) \left[\nabla_2^D \nabla_2^D \phi_2 + \nabla_1^D \nabla_1^D \phi_2 \right].\end{aligned}\quad (4.30)$$

Modal solutions of any BVP follow from the 1d and 2d fractal Helmholtz equations introduced above.

4.3 Elastodynamics of a fractal Timoshenko beam

Analogous results, also exhibiting self-consistency, were obtained in elastodynamics of a fractally structured Timoshenko beam [12]. First recall that such a beam model has two degrees of freedom (q_1, q_2) at each point: the transverse displacement $q_1 = w$ and the rotation $q_2 = \varphi$. In the mechanical approach the beam equation can be derived from the force and moment balance analysis. Thus, beginning with the expressions of shear force (V) and bending moment (M)

$$V = \kappa\mu A \left(\nabla_x^D w - \varphi \right), \quad M = -EI \nabla_x^D \varphi, \quad (4.31)$$

we find

$$\rho A \ddot{w} = \nabla_x^D V, \quad \rho I \ddot{\varphi} = V - \nabla_x^D M, \quad (4.32)$$

which lead to

$$\begin{aligned} \rho A \ddot{w} &= \nabla_x^D \left[\kappa\mu A \left(\nabla_x^D w - \varphi \right) \right], \\ \rho I \ddot{\varphi} &= \nabla_x^D \left(EI \nabla_x^D \varphi \right) + \kappa\mu A \left(\nabla_x^D w - \varphi \right). \end{aligned} \quad (4.33)$$

The kinetic energy is

$$T = \frac{1}{2} \rho \int_0^l \left[I (\dot{\varphi})^2 + A (\dot{w})^2 \right] dl_D, \quad (4.34)$$

while the potential energy is

$$\begin{aligned} U &= \frac{1}{2} \int_0^l \left[EI \left(\frac{\partial \varphi}{\partial l_D} \right)^2 + \kappa\mu A \left(\frac{\partial w}{\partial l_D} - \varphi \right)^2 \right] dl_D \\ &= \frac{1}{2} \int_0^l \left[EI c_1^{-2} (\varphi_{,x})^2 + \kappa\mu A (c_1^{-1} w_{,x} - \varphi)^2 \right] c_1 dx. \end{aligned} \quad (4.35)$$

Now, the Euler-Lagrange equations

$$\frac{\partial}{\partial t} \left[\frac{\partial L}{\partial \dot{q}_i} \right] + \sum_{j=1}^3 \frac{\partial}{\partial x_j} \left[\frac{\partial L}{\partial (q_{i,j})} \right] - \frac{\partial L}{\partial q_i} = 0 \quad (4.36)$$

result in the same as above.

In the case of elastostatics and when the rotational degree of freedom ceases to be independent ($\varphi = \partial w / \partial l_D = \nabla_x^D w$), we find the equation of a fractal Euler-Bernoulli beam

$$\nabla_x^D \nabla_x^D \left(EI \nabla_x^D \nabla_x^D w \right) = 0, \quad (4.37)$$

which shows that

$$M = EI \nabla_x^D \nabla_x^D w. \quad (4.38)$$

The relationship between the bending moment (M) and the curvature ($\nabla_x^D \nabla_x^D w$) still holds, while c_1 enters the determination of curvature ($\nabla_x^D \nabla_x^D w = c_1^{-1} (c_1^{-1} w_{,x})_{,x}$).

In a nutshell, the fractional power law of mass implies a fractal dimension of scale measure, so the derivatives involving spatial scales should be modified to incorporate such effect by postulating c_1, c_2, c_3 coefficients, according to the material body being embedded in a 1d, 2d, or 3d Euclidean space.

4.4 Fractal elastic solid under finite strains

To obtain the equations of motion for a fractal elastic solid under finite strains, we begin with Hamilton's Principle for the Lagrangian $\mathcal{L} = \mathcal{K} - \mathcal{E}$ of a fractal solid \mathcal{W} isolated from external interactions,

$$\delta \mathcal{I} = \delta \int_{t_1}^{t_2} [\mathcal{K} - \mathcal{E}] dt = 0, \quad (4.39)$$

where \mathcal{K} and \mathcal{E} are the kinetic and internal energies

$$\mathcal{K} = \frac{1}{2} \int_{\mathcal{W}} \rho v_i v_i dV_D \quad \mathcal{E} = \int_{\mathcal{W}} \rho e dV_D. \quad (4.40)$$

Thus, we have a functional, which can be rewritten in fractal space-time (e being the specific, per unit mass, internal energy density) as

$$0 = \delta \mathcal{I} = \delta \int_{t_1}^{t_2} \int_{\mathcal{W}} \left[\frac{1}{2} \rho v_k^2 - \rho e \right] dV_D dt = \delta \int_{t_1}^{t_2} \int_{\mathcal{W}} \left[\rho \frac{1}{2} v_k^2 - \rho e \right] dV_D dt. \quad (4.41)$$

Analogous to the strain of (3.4), the deformation gradient is

$$F_{kI} = \frac{1}{c_1^{(I)}} x_{k,I} = \nabla_I^D x_k. \quad (4.42)$$

Assuming that the specific energy density e depends only on the deformation gradient, and that ρ has no explicit dependence on time, leads to:

(i) the boundary conditions on

$$\partial \mathcal{W} \rho \frac{\partial e}{\partial F_{kI}} N_I = 0 \quad \text{or} \quad \delta x_k = 0 \quad \text{on} \quad \partial \mathcal{W}, \quad (4.43)$$

(ii) the kinematic constraints, $\delta x_k = 0$ at $t = t_1$ and $t = t_2$, which imply the equation governing motion in a fractal solid under finite strains

$$\nabla_I^D \left[\rho \frac{\partial e}{\partial F_{kI}} \right] - \rho \frac{dv_k}{dt} = 0 \quad \text{or} \quad \frac{1}{c_1^{(I)}} \frac{\partial}{\partial X_I} \left[\rho \frac{\partial e}{\partial F_{kI}} \right] - \rho \frac{dv_k}{dt} = 0. \quad (4.44)$$

Next, in fractal bodies without internal dissipation, e plays the role of a potential

$$T_{kI} = \rho \frac{\partial e}{\partial F_{kI}}, \quad (4.45)$$

where T_{kI} is the first Piola-Kirchhoff stress tensor, and (4.44) becomes

$$\nabla_I^D T_{kI} - \rho \frac{dv_k}{dt} = 0 \quad \text{or} \quad \frac{1}{c_1^{(I)}} T_{kI,I} - \rho \frac{dv_k}{dt} = 0. \quad (4.46)$$

Restricting the motion to small deformation gradients, T_{kI} becomes the Cauchy stress tensor and we recover the linear momentum equation (3.11). Generalizing this to the situation of \mathcal{W} interacting with the environment (i.e., subject to body forces) [35],

$$\delta (\mathcal{I} + W - \mathcal{P}) = 0, \quad (4.47)$$

we obtain

$$\nabla_I^D T_{kI} + \rho \left(b_k - \frac{dv_k}{dt} \right) = 0 \quad \text{or} \quad \frac{1}{c_1^{(I)}} T_{kI,I} + \rho \left(b_k - \frac{dv_k}{dt} \right) = 0. \quad (4.48)$$

In [24] we also considered one-dimensional models and obtained equations governing the nonlinear waves in such a solid. We showed that the equations can be solved by the method of characteristics in fractal space-time. We also studied shock fronts in linear viscoelastic solids under small strains. We showed that the discontinuity in stress across a shock front in a fractal medium is identical to the classical result.

5 Related topics

5.1 Extremum and variational principles in fractal bodies

Just like in preceding sections, the dimensional regularization approach can also be applied to other statements in continuum/solid mechanics involving integral relations. For example, the Maxwell-Betti reciprocity relation of linear elasticity $\int_{\partial W} t_i^* u_i dS_2 = \int_{\partial W} t_i u_i^* dS_2$ is generalized for fractal media to

$$\int_{\partial W} t_i^* u_i dS_d + \int_{\partial W} m_i^* \varphi_i dS_d = \int_{\partial W} t_i u_i^* dS_d + \int_{\partial W} m_i \varphi_i^* dS_d, \quad (5.1)$$

so as to read in \mathbb{E}^3 :

$$\int_{\partial W} t_i^* u_i c_2 dS_2 + \int_{\partial W} m_i^* \varphi_i c_2 dS_2 = \int_{\partial W} t_i u_i^* c_2 dS_2 + \int_{\partial W} m_i \varphi_i^* c_2 dS_2. \quad (5.2)$$

The reciprocity relation (5.1) is proved by appealing to the Green-Gauss theorem and the Hooke law ($\sigma_{ij} = C_{ijkl} \varepsilon_{kl}$), and proceeding just like in the conventional continuum elasticity. As an application, consider the classical problem of calculation of the reduction in volume ΔV of a linear elastic isotropic body (of bulk modulus κ) due to two equal, collinear, opposite forces F , separated by a distance L . Clearly, in the classical case, one does not need the micropolar term and, as discussed in [12], finds $\Delta V = FL/3\kappa$. On the other hand, for a fractal body, given the loading $\tau_{ij} = -p\delta_{ij}$ and $\mu_{ij} = 0$, the integrals involving scalar products of couple traction with rotation vanish, and we obtain

$$p \Delta V c_3 = p \frac{FL}{3\kappa} c_1. \quad (5.3)$$

Recalling (2.13) and assuming that the opposite forces are applied parallel to one of the axes of the coordinate system (say, x_k), yields $\Delta V = FLc_1/3\kappa c_3$. This can be evaluated numerically for a specific material according to (2.13).

Next, suppose we focus on situations where couple-stress effects are negligible. Then, we recall the concept of a *statically admissible field* as a tensor function $\sigma_{ij}(\mathbf{x})$, such that $\sigma_{ij} = \sigma_{ji}$ and $(F_k = \rho f_k)$

$$F_k + \nabla_l^D \sigma_{kl} = 0 \quad (5.4)$$

in W and the boundary conditions

$$\sigma_{kl} n_l = t_k \quad (5.5)$$

on ∂W_t . Similarly, we recall a *kinematically admissible displacement field* as a vector function $\mathbf{u}(\mathbf{x})$ satisfying the boundary conditions

$$u_i = f_i \quad (5.6)$$

on ∂W_u . We can now consider the *Principle of Virtual Work*: "The virtual work of the internal forces equals the virtual work of the external forces." Let $\sigma(\mathbf{x})$ be a statically admissible stress field, $\mathbf{u}(\mathbf{x})$ a kinematically admissible displacement field. Define $\varepsilon_{ij}(\mathbf{u}) = u_{(i,j)}$. Then

$$\int_W \sigma_{ij} \varepsilon_{ij} dV_D = \int_W F_i u_i dV_D + \int_{\partial W_t} t_i u_i dS_d + \int_{\partial W_u} \sigma_{ij} n_j f_i dS_d. \quad (5.7)$$

The proof follows by substitution from the fractional equation of static equilibrium and boundary conditions after integrating by parts, and using the Gauss theorem, all conducted over the fractal domain W . Of course, the above can be rewritten in terms of conventional integrals:

$$\int_W \sigma_{ij} \varepsilon_{ij} c_3 dV_3 = \int_W F_i u_i c_3 dV_3 + \int_{\partial W_t} c_2 t_i u_i c_2 dS_2 + \int_{\partial W_u} \sigma_{ij} n_j f_i c_2 dS_2. \quad (5.8)$$

In a similar way, we can adapt to fractal elastic bodies the Principle of Virtual Displacement, Principle of Virtual Stresses, Principle of Minimum Potential Energy, Principle of Minimum Complementary Energy, and related principles for elastic-plastic or rigid bodies.

Relation to other studies of complex systems: While the dimensional regularization has been employed for fractal porous media, the approach can potentially be extended to microscopically heterogeneous physical systems (made up

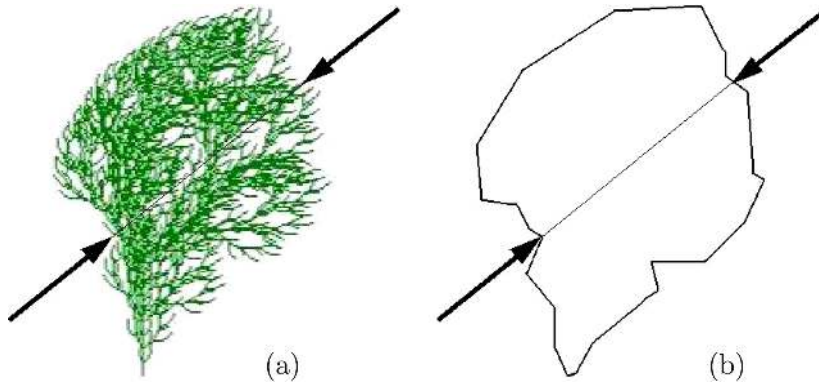


Fig. 7 (online colour at: www.zamm-journal.org) (a) A fractal body subjected to two equal, collinear, opposite forces F , and (b) its homogenized equivalent via dimensional regularization.

of many different micromechanical systems, having different physical properties, and interacting under the influence of different kinds of phenomena). In particular, it seems possible to generalize the foregoing developments in two ways:

(i) By taking as the starting point the "microscopic models" for interactions between the fluid flow and a deformable porous matrix [70–73] so as to obtain higher gradient fractal models.

(ii) By looking for physical systems which can be modelled at a microscopic level as first gradient continua and become higher gradient models after the dimensional regularization procedure has been applied [74–76].

Once higher gradient fractal models are obtained, it should be possible to generalize the results of [77–80] for second gradient nematic fluids (for which a clear micro-macro identification procedure seems not already clarified sufficiently), or for the equilibrium of liquid films and drops in [80] (which accounted for phase equilibrium in liquid films) or for liquid drops on walls, or, yet, for wave propagation phenomena [82].

5.2 Fracture in elastic-brittle fractal solids

5.2.1 General considerations

According to Griffith's theory of elastic-brittle solids, the strain energy release rate G is given by [36]

$$G = \frac{\partial W}{\partial A} - \frac{\partial \mathcal{E}^e}{\partial A} = 2\gamma, \quad (5.9)$$

where A is the crack surface area formed, W is the work performed by the applied loads, \mathcal{E}^e is the elastic strain energy, and γ is the energy required to form a unit of new material surface. The material parameter γ is conventionally taken as constant, but, given the presence of a randomly microheterogeneous material structure, its random field nature is sometimes considered explicitly [37, 38]. Recognizing that the random material structure also affects the elastic moduli (such as E), the computation of \mathcal{E}^e and G in (5.9) needs to be re-examined [38]; see also [39] in the context of paper mechanics. With reference to Fig. 7, we consider a 3d material body described by D and d , and having a crack of depth a and a fractal dimension DF .

Focusing on a fractal porous material, we have

$$U^e = \int_W \rho u dV_D = \int_W \rho u c_3 dV_3. \quad (5.10)$$

By revising Griffith's derivation for a fractal elastic material, we then obtain

$$U^e = \frac{\pi a^2 c_1^2 \sigma^2}{8\mu} (K + 1) c_3, \quad (5.11)$$

with ν being the Poisson ratio, and

$$K = \begin{cases} 3 - 4\nu & \text{for plane strain} \\ \frac{3 - \nu}{1 + \nu} & \text{for plane stress} \end{cases} \quad (5.12)$$

the Kolosov constant.

Dead-load conditions. Equation (5.9) becomes

$$G = \frac{\partial U^e}{\partial A} = 2\gamma. \quad (5.13)$$

If $A = 2a \times 1$, this gives the critical stress

$$\sigma_c = \sqrt{\frac{2\gamma E}{(1-\nu^2)\pi a c_3 c_1^2}}. \quad (5.14)$$

However, if the fracture surface is fractal of a dimension α , then we should use $\partial/\partial l_{DF}$ instead of $\partial/\partial a$. Now, since we have (note Fig. 8) $dl_{DF} = c_1 da$, the new partial derivative becomes

$$\frac{\partial}{\partial l_{DF}} = \frac{\partial}{c_1 \partial a}, \quad (5.15)$$

so that

$$\sigma_c = \sqrt{\frac{2\gamma E}{(1-\nu^2)\pi a c_3 c_1}}. \quad (5.16)$$

Fixed-grip conditions. We consider the case of a crack of depth a and width B in plane strain. In this case the displacement is constant (i.e., non-random), and the load is random. Now, only the second term in (5.9) remains, so that

$$G = -\frac{\partial \mathcal{E}^e(a)}{B \partial l_{DF}} = -\frac{\partial \mathcal{E}^e(a)}{B c_1 \partial a}. \quad (5.17)$$

5.2.2 Peeling a layer off a substrate

Dead-load conditions. As a specific case we take an Euler-Bernoulli beam, so that the strain energy is

$$\mathcal{E}(a) = \int_0^a \frac{M^2}{2IE} dx, \quad (5.18)$$

where a is crack length, M is bending moment, and I is beam's moment of inertia. Henceforth, we simply work with $a = A/B$, where B is the constant beam (and crack) width. In view of Clapeyron's theorem, the strain energy release rate may be written as

$$G = \frac{\partial \mathcal{E}}{B \partial a}. \quad (5.19)$$

For a layer modeled as a fractal Euler-Bernoulli beam (Sect. 4.3), we have

$$\mathcal{E}(a) = \int_0^a \frac{M^2}{2IE} dl_D = \int_0^a \frac{M^2}{2IE} c_1 dx, \quad (5.20)$$

so that

$$G = \frac{\partial \mathcal{E}}{c_1 B \partial a}. \quad (5.21)$$

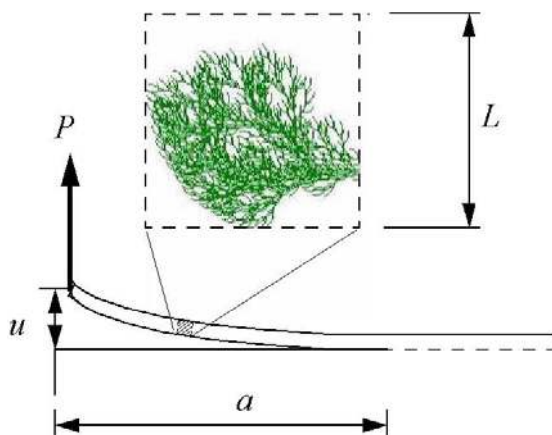


Fig. 8 (online colour at: www.zamm-journal.org) Fracture and peeling of a microbeam of thickness L off a substrate. A representative volume element dV_3 imposed by the pre-fractal structure characterized by upper cutoff scale L is shown. Thus, the beam is homogeneous above the length scale L . By introducing random variability in that structure, one obtains a random beam, see (5.22).

5.2.3 Generalization to a statistical ensemble

Now, if the beam's material is random, E is a random field parametrized by x , which we can write as a sum of a constant mean $\langle E \rangle$ and a zero-mean fluctuation $E'(\omega)$

$$E(\omega, x) = \langle E \rangle + E'(\omega, x) \quad \omega \in \Omega, \quad (5.22)$$

where ω is an elementary event in Ω , a sample space. Clearly, \mathcal{E} is a random integral, such that, for each and every realization $\omega \in \Omega$, we should consider

$$\mathcal{E}(a, E(\omega)) = \int_0^a \frac{M^2 c_1 dx}{2IE(\omega, x)}. \quad (5.23)$$

Upon ensemble averaging, this leads to an average energy

$$\langle \mathcal{E}(a, E) \rangle = \left\langle \int_0^a \frac{M^2 c_1 dx}{2I [\langle E \rangle + E'(\omega, x)]} \right\rangle. \quad (5.24)$$

In the conventional formulation of deterministic fracture mechanics, random microscale heterogeneities $E'(x, \omega)$ are disregarded, and (5.23) is evaluated by simply replacing the denominator by $\langle E \rangle$, so that

$$\mathcal{E}(a, \langle E \rangle) = \int_0^a \frac{M^2 c_1 dx}{2I \langle E \rangle}. \quad (5.25)$$

Clearly, this amounts to postulating that the response of an idealized homogeneous material is equal to that of a random one on average. To make a statement about $\langle \mathcal{E}(a, E) \rangle$ versus $\mathcal{E}(a, \langle E \rangle)$, and about $\langle G(E) \rangle$ versus $G(\langle E \rangle)$, first, note the random field E is positive-valued almost surely. Then, Jensen's inequality yields a relation between harmonic and arithmetic averages of the random variable $E(\omega)$

$$\frac{1}{\langle E \rangle} \leq \left\langle \frac{1}{E} \right\rangle, \quad (5.26)$$

whereby the x -dependence is immaterial in view of the assumed wide-sense stationary of field E . With (5.24) and (5.25), and assuming that the conditions required by Fubini's theorem are met, this implies that

$$\mathcal{E}(a, \langle E \rangle) = \int_0^a \frac{M^2 c_1 dx}{2I \langle E \rangle} \leq \int_0^a \frac{M^2 c_1}{2I} \left\langle \frac{1}{E} \right\rangle dx = \left\langle \int_0^a \frac{M^2 c_1 dx}{2IE(\omega, x)} \right\rangle = \langle \mathcal{E}(a, E) \rangle. \quad (5.27)$$

Now, defining the strain energy release rate $G(a, \langle E \rangle)$ in a reference material specified by $\langle E \rangle$, and the strain energy release rate $\langle G(a, E) \rangle$ properly ensemble averaged in the random material $\{E(\omega, x); \omega \in \Omega, x \in [0, a]\}$

$$G(a, \langle E \rangle) = \frac{\partial \mathcal{E}(a, \langle E \rangle)}{B c_1 \partial a}, \quad \langle G(a, E) \rangle = \frac{\partial \langle \mathcal{E}(a, E) \rangle}{B c_1 \partial a}, \quad (5.28)$$

and noting that the side condition is the same in both cases

$$\mathcal{E}(a, \langle E \rangle) |_{a=0} = 0, \quad \langle \mathcal{E}(a, E) \rangle |_{a=0} = 0, \quad (5.29)$$

we find

$$G(a, \langle E \rangle) \leq \langle G(a, E) \rangle. \quad (5.30)$$

This provides a formula for the ensemble average G under dead-load conditions using deterministic fracture mechanics for Euler-Bernoulli beams made of fractal random materials.

Just like in the case of non-fractal materials [38], the inequality (5.30) shows that G computed under the assumption that the random material is directly replaced by a homogeneous material ($E(x, \omega) = \langle E \rangle$), is lower than G computed with E taken explicitly as a spatially varying material property.

Fixed-grip conditions. On account of (2.11), assuming that there is loading by a force P at the tip, we obtain

$$G = -\frac{u}{2Bc_1} \frac{\partial P}{\partial a}. \quad (5.31)$$

Take now a cantilever beam problem implying $P = 3uEI/(c_1a)^3$. Then, we find

$$\langle G \rangle = -\frac{u}{2Bc_1} \left\langle \frac{\partial P}{\partial a} \right\rangle = -\frac{u}{2Bc_1} \frac{\partial \langle P \rangle}{\partial a} = \frac{9u^2 I \langle E \rangle}{2B(c_1a)^4}. \quad (5.32)$$

Since the load – be it a force and/or a moment – is always proportional to E , this indicates that G can be computed by direct ensemble averaging of E under fixed-grip loading, and, indeed, the same conclusion carries over to Timoshenko beams. This analysis may be extended to mixed-loading conditions and stochastic crack stability by generalizing the study of non-fractal, random beams carried out in [12].

5.2.4 Studies of cracks with fractal profiles

A separate line of studies has – indeed, a spate of works – originated from the 1984 observation that cracks (i.e. crack profiles) in many materials display fractality [40]. Of many studies that have aimed to generalize fracture mechanics we list [41–45]. One particularly promising line of research on fractal cracks in non-fractal materials is due to Wnuk & Yavari [46, 50, 57–59]: the basic idea has been to adapt the existing solutions for the singular stress field in the vicinity of a fractal crack tip: a smooth crack is embedded in a singular stress field for which the order of singularity is adjusted to match exactly the one obtained from the analyses pertaining to the fractal crack. The embedded crack model is based on the fact that the order of singularity for near-tip stresses changes from $r^{-1/2}$ for a smooth cracks to $r^{-\alpha}$ for a rough crack. Therefore, the exponent α can be used as a measure of degree of roughness and it is related to the crack's fractal dimension $D \in (1, 2)$ by $\alpha = (2 - D)/2$. Additionally, the material ductility is measured by another index (ρ) which can be related either to the microstructural parameters by $\rho = R_{init}/\Delta$ (where R_{init} is the length of the cohesive zone at the onset of crack growth while Δ is the size of the process zone adjacent to the crack front) or to the macro material parameters by $\rho = 1 + \varepsilon_{pl}^f/\varepsilon_Y$, where ε_Y is the yield strain and ε_{pl}^f is the plastic component of the strain at fracture.

5.3 Turbulence in fractal porous media

Here we examine the basic equations governing turbulent flow in fractal porous media. Following the classical approach, we begin by assuming a split of the velocity, stress, energy density and heat flux fields into their mean and fluctuating parts such as expressed for velocity by

$$v_i = \langle v_i \rangle + v'_i, \quad \langle v'_i \rangle = 0. \quad (5.33)$$

Recalling that the classical case of flows in Euclidean media involves three corrections [11]

$$\begin{aligned} \sigma_{kl}^* &= \sigma_{kl} - \rho \langle v'_k v'_l \rangle, \\ u^* &= \langle u \rangle + \frac{1}{2} \langle v'_i v'_i \rangle, \\ q_l^* &= q_l - \langle v'_k \sigma'_{kl} \rangle + \rho \langle u' v'_l \rangle + \rho \langle v'_k v'_k v'_l \rangle / 2, \end{aligned} \quad (5.34)$$

the most famous being the Reynolds stress σ_{ij}^* , we inquire whether turbulence in fractal porous media will have the same expressions as (5.36). To this end, introducing (5.35) into (5.36), and carrying out the averaging, we obtain

$$\nabla_k^D \langle v_k \rangle = 0, \quad (5.35)$$

showing that the secular part of the velocity field is subject to the same continuity equation.

Next, the integral form of the balance of linear momentum in any medium of Euclidean structure, with respect to an observer at rest, is known to have this form [28]

$$\int_W \rho v_{k,0} dV_3 = \int_{\partial W} [\sigma_{kl} - \rho v_k v_l] n_l dS_2, \quad (5.36)$$

where \cdot_0 stands for the partial time derivative $\partial/\partial t$. Now, considering a fractal medium, we have

$$\int_W \rho v_{k,0} dV_D = \int_{\partial W} [\sigma_{kl} - \rho v_k v_l] n_l dS_d. \quad (5.37)$$

Assuming the velocity field (5.33) and an analogous split of the stress field, upon averaging, we obtain

$$\int_W \rho \langle v_k \rangle_0 dV_D = \int_{\partial W} [\langle \sigma_{kl} \rangle - \rho (\langle v_k \rangle \langle v_l \rangle + \langle v'_k v'_l \rangle)] n_l dS_d, \quad (5.38)$$

which shows that (5.37) retains its form for the secular parts of velocity and stress fields, providing we take σ_{kl}^* in place of the mean stress $\langle \sigma_{kl} \rangle$

$$\sigma_{kl}^* = \langle \sigma_{kl} \rangle - \rho \langle v'_k v'_l \rangle. \quad (5.39)$$

Thus, apparently, $-\rho \langle v'_k v'_l \rangle$ is the Reynolds stress correction just as in the classical theories for non-fractal geometries. To verify that conclusion, we will now transform (3.4) to a local (differential) form. To this end, by using the Green-Gauss theorem for fractals (2.26), (5.38) transforms to

$$\int_W \rho \langle v_k \rangle_0 dV_D = \int_W \nabla_l^D \{ [\langle \sigma_{kl} \rangle - \rho (\langle v_k \rangle \langle v_l \rangle + \langle v'_k v'_l \rangle)] \} dV_D, \quad (5.40)$$

which leads to

$$\rho [\langle v \rangle_k \cdot_0 + \langle v \rangle_l \nabla_l^D \langle v \rangle_k] = \nabla_l^D \left[\langle \sigma_{kl} \rangle - \rho \langle \overline{v'_k v'_l} \rangle \right], \quad (5.41)$$

instead of the conventional relation

$$\rho [\langle v \rangle_k \cdot_0 + \langle v \rangle_l \nabla_l \langle v \rangle_k] = \left[\langle \sigma_{kl} \rangle - \rho \langle \overline{v'_k v'_l} \rangle \right]_{,l}. \quad (5.42)$$

This confirms that the Reynolds stress (σ_{kl}^*) can be simply written as $\sigma_{kl}^* = \langle \sigma_{kl} \rangle - \rho \langle v'_k v'_l \rangle$, providing the spatial gradient is interpreted as ∇_l^D . This result is not obtained with the original calculus of Tarasov, thus showing that the calculus based on product measures is more consistent. This remark is amplified by considering the energy conservation equation which gives, just like in the case of non-fractal media,

$$\begin{aligned} u^* &= \langle u \rangle - \langle v'_k v'_k \rangle / 2, \\ q_l^* &= \langle q_l \rangle - \langle v'_k \sigma'_{kl} \rangle + \rho \langle u' v'_l \rangle + \rho \langle v'_k v'_k v'_l \rangle / 2. \end{aligned} \quad (5.43)$$

5.4 Balankin's formulation

In two recent papers [51, 52] a formulation of fluid flow in fractal porous media, similar to ours, yet claimed to be superior, has been suggested. The key points to note are:

(i) Those authors adopted c_1 in this form: $c_1 = (x/l_0 + 1)^{\zeta-1}$, where l_0 is the lower cut-off. However, there is no essential difference from our $c_1 = [(L-x)/L]^{\zeta-1} = (1-x/L)^{\zeta-1}$, since both formulas reflect the same power scaling of mass. In effect, the product measure framework does not change.

(ii) Their dV_D has been postulated in the form: $dV_D = c_1 dx_1 c_2 dS_2$, which refers c_2 (and, hence, the surface fractal dimension d_2) to a specific fractal plane. Furthermore, for a surface $S_2^{(k)}$ orthogonal to x_k , having a fractal dimension $d_2^{(k)}$ ($k \neq i, j$), they set $c_2 = c_1(d_2^{(k)}/2, x_i) c_1(d_2^{(k)}/2, x_j)$. However, this implies ambiguity and, hence, non-uniqueness of the specification of c_3 since $c_3 = c_1(d_1^{(k)}, x_k) c_1(d_2^{(k)}/2, x_i) c_1(d_2^{(k)}/2, x_j) = c_1(d_1^{(j)}, x_j) c_1(d_2^{(j)}/2, x_i) c_1(d_2^{(j)}/2, x_k)$ while $d_1^{(j)} \neq d_2^{(k)}/2$. On the other hand, our product measure formulation provides a unique and consistent expression of the c_1 , c_2 , and c_3 coefficients.

(iii) Employing a Hausdorff derivative introduced in [53], they have adopted:

$$\frac{d^H f}{dx^\zeta} = \lim_{x \rightarrow x'} \frac{f(x') - f(x)}{x'^\zeta - x^\zeta}. \quad (5.44)$$

This can actually be shown to lead to

$$\nabla^H = \frac{d^H f}{dx^\zeta} = \frac{1}{c_1} \frac{df}{dx}, \quad (5.45)$$

with $c_1 = (x/l_0 + 1)^{\zeta-1}$ as given in (i) above. On account of (2.25), this is a re-writing of our derivative ∇^D .

(iv) A consideration of angular momentum balance leading to a loss of symmetry of stress tensor in an equivalent continuum has not been undertaken. Indeed, in view of our Sect. 3.3, the governing equations of flow in fractal porous media studied by Balankin & Elizarraraz as well as that in Sect. 5.3 will have to be augmented by micropolar quantities.

5.5 Other fractal and fractional calculus mechanics models

In a series of works [54–56] a new approach to self-similar harmonic interparticle interactions has been advanced. First, starting with a linear chain model, this has led to a self-similar Laplacian which, in the continuum limit, takes the form of a combination of fractional integrals. Then the Hooke law becomes a non-local convolution with the elastic modulus function being a power-law kernel. The authors identify an anomalous behavior of the elastic modulus function reflecting a regime of critically slowly decreasing interactions. As another application, this Laplacian was employed to study a self-similar diffusion, where solutions have been found to be Lévy-stable distributions with infinite variances [57].

Development of a mechanical theory of fractals (and non-smooth bodies in general) on the basis of differential spaces of Sikorski has been undertaken in [58]. First a configuration space has been identified and then an extended form of the principle of virtual work has been formulated, which, in turn, allowed a definition of generalized force and stress for fractal objects, leading to a numerical determination of stiffness matrices of some common fractals. This approach has led to a study of structural self-similarity [59, 60], its most interesting feature being that the stabilized properties are obtained only after a finite number of iterations.

The past two decades have seen a marked output of works on fractional calculus in continuum mechanics. The typical motivation is the interest in generalizing the constitutive equation for viscoelasticity or diffusion (e.g. heat conduction) via fractional derivatives or integrals in place of Newtonian ones; of the vast literature in this area we only cite [62–68]. All these studies, however, are characterized by the lack of (any clear) connection to the actual material microstructure, be it fractal or non-fractal, a remark which is not meant as a criticism but a statement of an outstanding challenge in mechanics.

6 Closure

Fractals are abundant in nature. Since the mechanics of fractal media is still in its infancy, it is important to develop methods to model fractal media. In this paper, we showed how fundamental balance laws for fractals can be developed using a homogenization method called dimensional regularization. The basis of this method is to express the balance laws for fractal media in terms of fractional integrals and, then, convert them to integer-order integrals in conventional (Euclidean) space. Dimensional regularization produces balance laws that are expressed in continuous form, thereby simplifying their mathematical manipulation. Of particular importance are the definitions of fractal space and time derivatives required to preserve mathematical consistency. Following an account of this method, we showed how to develop balance laws of fractal media (continuity, linear and angular momenta, first and second law of thermodynamics) and discussed wave equations in several settings (1d and 3d wave motions, fractal Timoshenko beam, and elastodynamics under finite strains). We also showed that angular momentum balance cannot be satisfied unless the stress tensor is asymmetric. Therefore, the introduction of fractal effects into anisotropic problems requires the adoption of a non-classical elastic constitutive model, the Cosserat model, for the balance laws to be satisfied. We discussed extremum and variational principles, fracture mechanics, and equations of turbulence in fractal media. In all the cases, the derived equations for fractal media depend explicitly on fractal dimensions and reduce to conventional forms for continuous media with Euclidean geometries upon setting the dimensions to integers. The fractal model discussed is useful for solving complex mechanics problems involving fractal materials composed of microstructures of inherent length scale, generalizing the universally applied classical theory of elastodynamics for continuous bodies. This model is a solid foundation upon which we can study (thermo)mechanical phenomena involving fractals analytically and computationally.

Acknowledgements This work was made possible by the support from Sandia-DTRA (grant HDTRA1-08-10-BRCWMD) and the NSF (grant CMMI-1030940). Also, the support of the first author as Timoshenko Distinguished Visitor in the Division of Mechanics and Computation, Stanford University, is gratefully acknowledged.

References

- [1] B. Mandelbrot, *The Fractal Geometry of Nature* (W.H. Freeman, New York, 1982).
- [2] M. F. Barnsley, *Fractals Everywhere* (Morgan Kaufmann, San Francisco, CA, 1993).
- [3] A. Le Méhauté, *Fractal Geometry: Theory and Applications* (CRC Press, Boca Raton, FL, 1991).
- [4] H. M. Hastings and G. Sugihara, *Fractals: A User's Guide for the Natural Sciences* (Oxford Science Publications, Oxford, 1993).
- [5] K. Falconer, *Fractal Geometry: Mathematical Foundations and Applications* (J. Wiley, Chichester, 2003).
- [6] V. E. Tarasov, Fractional hydrodynamic equations for fractal media, *Ann. Phys. (New York)* **318**(2), 286–307 (2005).
- [7] V. E. Tarasov, Wave equation for fractal solid string, *Mod. Phys. Lett. B* **19**(15), 721–728 (2005).
- [8] M. Ostoja-Starzewski, Towards thermomechanics of fractal media, *Z. Angew. Math. Phys.* **58**(6), 1085–1096 (2007).
- [9] M. Ostoja-Starzewski, Extremum and variational principles for elastic and inelastic media with fractal geometries, *Acta Mech.* **205**, 161–170 (2009).
- [10] M. Ostoja-Starzewski, On turbulence in fractal porous media, *Z. Angew. Math. Phys.* **59**(6), 1111–1117 (2008).
- [11] H. Joumaa and M. Ostoja-Starzewski, On the wave propagation in isotropic fractal media, *Z. Angew. Math. Phys.* **62**, 1117–1129 (2011).
- [12] J. Li and M. Ostoja-Starzewski, Fractal materials, beams and fracture mechanics, *Z. Angew. Math. Phys.* **60**, 1–12 (2009).
- [13] G. Jumarie, Table of some basic fractional calculus formulae derived from a modified Riemann-Liouville derivative for non-differentiable functions, *Appl. Math. Lett.* **22**(3), 378–385 (2009).
- [14] V. E. Tarasov, Continuous medium model for fractal media, *Phys. Lett. A* **336**, 167–174 (2005).
- [15] V. E. Tarasov, *Fractional Dynamics: Applications of Fractional Calculus to Dynamics of Particles, Fields and Media* (Springer, Berlin, Heidelberg, New York, 2010).
- [16] J. C. Collins, *Renormalization* (Cambridge University Press, Cambridge, 1984).
- [17] J. Li and M. Ostoja-Starzewski, Fractal solids, product measures and fractional wave equations, *Proc. R. Soc. Lond. A* **465**, 2521–2536 (2009); Errata (2010).
- [18] J. Li and M. Ostoja-Starzewski, Fractal Solids, Product Measures and Continuum Mechanics, Chap. 33 in: *Mechanics of Generalized Continua: One Hundred Years After the Cosserats*, edited by G. A. Maugin and A. V. Metrikine (Springer, Berlin, Heidelberg, New York, 2010), pp. 315–323.
- [19] J. Li and M. Ostoja-Starzewski, Micropolar continuum mechanics of fractal media (A.C. Eringen special issue), *Int. J. Eng. Sci.* **49**, 1302–1310 (2011).
- [20] J. Ignaczak and M. Ostoja-Starzewski, *Thermoelasticity with Finite Wave Speeds* (Oxford University Press, Oxford, 2009).
- [21] R. Temam and A. Miranville, *Mathematical Modeling in Continuum Mechanics* (Cambridge University Press, Cambridge, 2005).
- [22] G. Jumarie, On the representation of fractional Brownian motion as an integral with respect to $(dt)^a$, *Appl. Math. Lett.* **18**, 739–748 (2005).
- [23] A. Carpinteri, B. Chiaia, and P. A. Cornetti, A disordered microstructure material model based on fractal geometry and fractional calculus, *Z. Angew. Math. Phys.* **84**, 128–135 (2004).
- [24] P. N. Demmie and M. Ostoja-Starzewski, Waves in fractal media, *J. Elast.* **104**, 187–204, 2011.
- [25] K. B. Oldham and J. Spanier, *The Fractional Calculus* (Academic Press, San Diego, 1974).
- [26] M. Ostoja-Starzewski, Electromagnetism on anisotropic fractal media, *Z. Angew. Math. Phys.*, online (2012).
- [27] D. Stoyan and H. Stoyan, *Fractals, Random Shapes and Point Fields* (John Wiley & Sons, Chichester, 1994).
- [28] H. Ziegler, *An Introduction to Thermomechanics* (North-Holland, Amsterdam, 1983).
- [29] A. Carpinteri and N. Pugno, Are scaling laws on strength of solids related to mechanics or to geometry? *Nature Mater.* **4**, 421–423 (2005).
- [30] W. Nowacki, *Theory of Asymmetric Elasticity* (Pergamon Press, Oxford, 1986); (PWN – Polish Sci. Publ., Warsaw, 1986).
- [31] H. Joumaa, M. Ostoja-Starzewski, and P. N. Demmie, Elastodynamics in micropolar fractal solids, *Math. Mech. Solids*, online doi: 10.1177/1081286512454557 (2012).
- [32] H. Joumaa and M. Ostoja-Starzewski, On the dilatational wave motion in anisotropic fractal solids (C. Christov special issue), *Math. Comp. in Simulation*, in review.
- [33] K. F. Graff, *Wave Motion in Elastic Solids* (Dover Publ., New York, 1975).
- [34] T. J. R. Hughes, *The Finite Element Method* (Dover Publ., New York, 2000).
- [35] C. Rymarz, *Mechanics of Continuous Media* (PWN – Polish Sci. Publ., Warsaw, 1993).
- [36] E. E. Gdoutos, *Fracture Mechanics: an Introduction*, (Kluwer Academic Publishers, Dordrecht, 1993).
- [37] M. Ostoja-Starzewski, Microstructural Randomness and Scaling in Mechanics of Materials, (CRC Press, Boca Raton, 2008).
- [38] M. Ostoja-Starzewski, Fracture of brittle micro-beams, *ASME J. Appl. Mech.* **71**, 424–427 (2004).
- [39] A. S. Balankin, O. Susarrey, C. A. Mora Santos, J. Patino, A. Yogues, and E. I. García, Stress concentration and size effect in fracture of notched heterogeneous material, *Phys. Rev. E* **83**, 015101(R) (2011).
- [40] B. B. Mandelbrot, D. E. Passoja, and A. J. Paullay, Fractal character of fracture surfaces of metals, *Nature* **308**, 721–722 (1984).
- [41] A. M. Brandt and G. Prokopski, On the fractal dimension of fracture surfaces of concrete elements, *J. Mater. Sci.* **28**, 4762–4766 (1993).
- [42] M. A. Issa, M. A. Issa, Md. S. Islam, and A. Chudnovsky, Fractal dimension – a measure of fracture roughness and toughness of concrete, *Eng. Fract. Mech.* **70**, 125–137 (2003).
- [43] F. M. Borodich, Fractals and fractal scaling in fracture mechanics, *Int. J. Fract.* **95**(1–4), 239–259, (1999).
- [44] A. Carpinteri, Scaling laws and renormalization groups for strength and toughness of disordered materials, *Int. J. Solids Struct.* **31**(3), 291–302 (1994).

- [45] A. Carpinteri and B. Chiaia, Multifractal scaling laws in the breaking behaviour of disordered materials, *Chaos, Solitons, Fractals* **8**(2) 135–150 (1997).
- [46] M. P. Wnuk and A. Yavari, On estimating stress intensity factors and modulus of cohesion for fractal cracks, *Eng. Fract. Mech.* **70**(13), 1659–1674 (2003).
- [47] M. P. Wnuk and A. Yavari, A correspondence principle for fractal and classical cracks, *Eng. Fract. Mech.* **72**(18), 2744–2757 (2005).
- [48] M. P. Wnuk and A. Yavari, Discrete fractal fracture mechanics, *Eng. Fract. Mech.* **75**(5), 1127–1142 (2008).
- [49] M. P. Wnuk and A. Yavari, A discrete cohesive model for fractal cracks, *Eng. Fract. Mech.* **76**(4), 1127–1142 (2009).
- [50] H. Khezzadeh, M. P. Wnuk, and A. Yavari, Influence of material ductility and crack surface roughness on fracture instability, *J. Phys. D, Appl. Phys.* **44**, 395302 (22p) (2011).
- [51] A. S. Balankin and B. E. Elizarraraz, Hydrodynamics of fractal continuum flow, *Phys. Rev. E* **85**, 025302(R) (2012).
- [52] A. S. Balankin and B. E. Elizarraraz, Map of fluid flow in fractal porous medium into fractal continuum flow, *Phys. Rev. E* **85**, 0256314(R) (2012).
- [53] W. Chen, Time-space fabric underlying anomalous diffusion, *Chaos Solitons Fractals* **28**, 923–929 (2006).
- [54] T. M. Michelitsch, G. A. Maugin, F. C. G. A. Nicolleau, A. F. Nowakowski, and S. Derogar, Dispersion relations and wave operators in self-similar quasi-continuous linear chains, *Phys. Rev. E* **80**, 011135 (2009).
- [55] T. M. Michelitsch, G. A. Maugin, M. Rahman, S. Derogar, A. F. Nowakowski, and F. C. G. A. Nicolleau, An approach to generalized one-dimensional self-similar elasticity, *Int. J. Eng. Sci.* **61**, 103–111 (2012).
- [56] T. M. Michelitsch, G. A. Maugin, M. Rahman, S. Derogar, A. F. Nowakowski, and F. C. G. A. Nicolleau, A self-similar field theory for 1D linear elastic continua and some applications to dynamic problems of wave propagation and diffusion, *Eur. J. Appl. Math.*, in press (2012).
- [57] T. M. Michelitsch, The self-similar field and its application to a diffusion problem, *J. Phys. A, Math. Theor.* **44**, 4665206 (2011).
- [58] M. Epstein and J. Śniatycki, Fractal mechanics, *Physica D* **220**, 54–68 (2006).
- [59] M. Epstein and J. Śniatycki, Fractal mechanics, *Int. J. Solids Struct.* **45**, 3238–3254 (2008).
- [60] M. Epstein and J. Śniatycki, Fractal elements, *JoMMS* **4**(5), 781–797 (2009).
- [61] E. Baskin and A. Iomin, Electrostatics in fractal geometry: Fractional calculus approach, *Chaos Solitons Fractals* **44**, 335–341 (2011).
- [62] R. L. Bagley and P. J. Torvik, A theoretical basis for the application of fractional calculus to viscoelasticity, *J. Rheol.* **27**, 201 (1983).
- [63] Y. A. Rossikhin, Reflections on two parallel ways in the progress of fractional calculus in mechanics of solids, *Appl. Mech. Rev.* **63**, 010701 (2010).
- [64] F. Mainardi, *Fractional Calculus and Waves in Linear Viscoelasticity* (Imperial College Press, London, 2010).
- [65] Y. Z. Povstenko, Fractional heat conduction equation and associated thermal stresses, *J. Thermal Stresses* **28**, 83–102 (2005).
- [66] H. H. Hilton, Generalized fractional derivative anisotropic viscoelastic characterization, *Materials* **5**, 169–191 (2012).
- [67] C. S. Drapaca and S. Sivaloganathan, A fractional model of continuum mechanics, *J. Elast.* **107**(2), 105–123 (2012).
- [68] C. M. Ionescu, W. Kosiński, and R. S. De Keyser, Viscoelasticity and fractal structure in a model of human lungs, *Arch. Mech.* **62**(1), 21–48 (2010).
- [69] A. C. Eringen, *Microcontinuum Field Theories* (Springer, Berlin, Heidelberg, New York, 1999).
- [70] G. Sciarra, F. dell’Isola, and O. Coussy, Second gradient poromechanics, *Int. J. Solids Struct.* **44**, 6607–6629 (2007).
- [71] G. Sciarra, F. dell’Isola, and K. Hutter, Dilatational and compacting behavior around a cylindrical cavern leached out in a solid-fluid elastic rock salt, *Int. J. Geomech.* **5**, 233–243 (2005).
- [72] G. Sciarra, F. dell’Isola, and K. Hutter, A solid-fluid mixture model allowing for solid dilatation under external pressure, *Contin. Mech. Thermodyn.* **13**, 287–306 (2001).
- [73] G. Sciarra, F. Dell’Isola, N. Ianiro, and A. Madeo, A variational deduction of second gradient poroelasticity – I: General theory, *J. Mech. Math. Struct.* **3**, 507–526 (2008).
- [74] J. Alibert, P. Seppecher, and F. dell’Isola, Truss modular beams with deformation energy depending on higher displacement gradients, *Math. Mech. Solids* **8**, 51–73 (2003).
- [75] A. Carcaterra and A. Akay, Theoretical foundations of apparent-damping phenomena and nearly irreversible energy exchange in linear conservative systems, *J. Acoust. Soc. Am.* **121**(4), 1971–1982 (2007).
- [76] A. Carcaterra and A. Akay, Dissipation in a finite-size bath, *Phys. Rev. E* **84**, 011121 (2011).
- [77] P. Seppecher, Thermodynamique des zones capillaires, *Ann. Phys. (France)* **13**, 13–22 (1988).
- [78] P. Seppecher, Etude des conditions aux limites en théorie du second gradient: cas de la capillarité, *C.R. Acad. Sci. II* **309**, 497–502, (1989).
- [79] P. Seppecher, Equilibrium of a Cahn and Hilliard fluid on a wall: Influence of the wetting properties of the fluid upon the stability of a thin liquid film, *Eur. J. Mech. B, Fluids* **12**(1), 69–84 (1993).
- [80] P. Seppecher, A numerical study of a moving contact line in Cahn-Hilliard theory, *Int. J. Eng. Sci.* **34**(9), 977–992 (1996).
- [81] P. Seppecher, Second-Gradient Theory: Application to Cahn-Hilliard Fluids, in: *Continuum Thermomechanics: The Art and Science of Modeling Matter’s Behaviour*, edited by G. A. Maugin et al. (Kluwer, Dordrecht, 2000), pp. 43–54.
- [82] F. dell’Isola, A. Madeo, and L. Placidi, Linear plane wave propagation and normal transmission and reflection at discontinuity surfaces in second gradient 3D continua, *Z. Angew. Math. Mech.* **92**(1), 52–71 (2012).